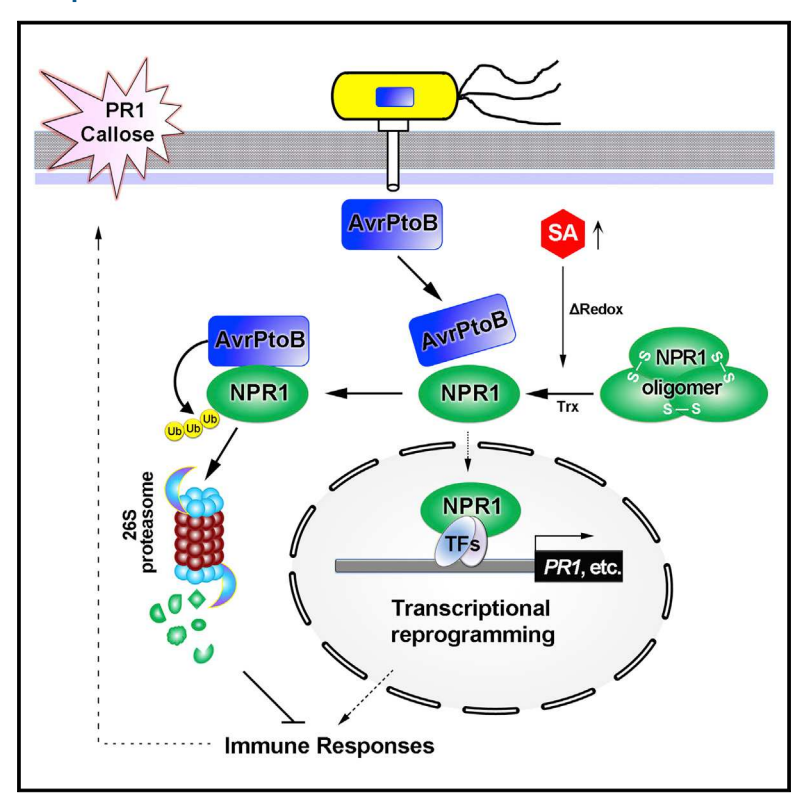
Cell Host & Microbe

A Bacterial Type III Effector Targets the Master Regulator of Salicylic Acid Signaling, NPR1, to Subvert Plant Immunity

Graphical Abstract



Authors

Huan Chen, Jian Chen, Min Li, ..., Marc T. Nishimura, Fengquan Liu, Zheng Qing Fu

Correspondence

fqliu20011@sina.com (F.L.), zfu@mailbox.sc.edu (Z.Q.F.)

In Brief

NPR1, as the key transcriptional regulator of salicylic acid signaling, plays a pivotal role in plant local and systemic immunity. Chen et al. find that *Pseudomonas* syringae type III effector AvrPtoB directly targets the activated form of NPR1 for ubiquitination-mediated degradation to inhibit target gene expression, thereby dampening plant immunity.

Highlights

- Salicylic acid (SA) promotes the interaction between NPR1 and AvrPtoB
- AvrPtoB facilitates NPR1 poly-ubiquitination and degradation via the 26S proteasome
- NPR1 acts as an important player in MAMP-triggered immunity
- AvrPtoB disrupts SA signaling, MAMP-triggered immunity, and systemic acquired resistance







A Bacterial Type III Effector Targets the Master Regulator of Salicylic Acid Signaling, NPR1, to Subvert Plant Immunity

Huan Chen,^{1,2} Jian Chen,^{1,2} Min Li,² Ming Chang,^{1,2} Kaimei Xu,² Zhenhua Shang,² Yi Zhao,^{1,2} Ian Palmer,² Yuqiang Zhang,^{2,3} Jon McGill,² James R. Alfano,⁴ Marc T. Nishimura,⁵ Fengquan Liu,^{1,*} and Zheng Qing Fu^{2,6,*}

SUMMARY

Most plant bacterial pathogens rely on type III effectors to cause diseases. Although it is well known that the plant hormone salicylic acid (SA) plays an essential role in defense, whether the master regulator of SA signaling, NPR1, is targeted by any plant pathogen effectors is unknown. SA facilitates the reduction of cytosolic NPR1 oligomers into monomers, which enter the nucleus and function as transcriptional coactivators of plant defense genes. We show that SA promotes the interaction between the Pseudomonas syringae type III effector AvrPtoB and NPR1. In the presence of SA, AvrPtoB mediates the degradation of NPR1 via the host 26S proteasome in a manner dependent on AvrPtoB's E3 ligase activity. Intriguingly, we found that NPR1 plays an important role in MAMP-triggered immunity (MTI), inducing the expression of MTI marker genes. Thus, this work uncovers a strategy in which AvrPtoB targets NPR1 and represses NPR1-dependent SA signaling, thereby subverting plant innate immunity.

INTRODUCTION

Many plant and animal bacterial pathogens use the type III secretion system to deliver type III effectors into their host cells in order to establish infection (Galan and Collmer, 1999). Different pathovars of the gram-negative plant bacterial pathogen *Pseudomonas syringae* inject into plant cells type III effectors belonging to about 57 families (Lindeberg et al., 2012). The major function of these type III effectors is to suppress plant innate immunity (Jones and Dangl, 2006; Fu et al., 2007; Block et al., 2008). Despite their sessile nature and lack of circulation system, plants have developed elegant strategies to defend themselves against pathogen infection. As the first layer of defense, plants utilize a large number of transmembrane receptor-

like kinases (RLKs) that function as pattern recognition receptors (PRRs) to perceive many conserved microbial molecules called microbe-associated molecular patterns (MAMPs), such as flagellin, elongation factor Tu (EF-Tu), fungal chitin, and glucan (Boller and Felix, 2009). These MAMPs can activate broad-spectrum immune responses called MAMP-triggered immunity (MTI). The brassinosteroid receptor-associated kinase 1 (BAK1) interacts with the flagellin receptor FLS2 or EF-Tu receptor EFR, and functions as an adaptor or a co-receptor to regulate PRR-dependent innate immunity (Sun et al., 2013). In order to cause diseases, plant pathogens, including fungi, oomycetes, and bacteria, deliver effectors into plant cells to suppress MTI and these effectors collectively cause diseases (Jones and Dangl, 2006). As an adaption to effector-triggered susceptibility, plants developed a robust second layer of the innate immune system termed effector-triggered immunity (ETI). ETI is triggered by disease resistance (R) proteins, mostly classified as nucleotide-binding site leucine-rich repeat (NBS-LRR) proteins, after direct or indirect detection of pathogen effectors. ETI is characterized by a robust defense output, often associated with rapid, programmed cell death, known as the hypersensitive response, to restrict pathogen propagation (Wu et al., 2014).

Plant innate immunity activates a set of signaling cascades, involving typical early immune responses, such as mitogen-activated protein kinase activation, reactive oxygen species production, marker gene expression, and later immune responses, such as callose deposition at cell walls and synthesis of pathogenesis-related (PR) proteins (Tsuda and Katagiri, 2010). Plant innate immunity, initiated from local tissues by virulent and avirulent pathogens, primes systemic defense by long-distance intercellular communications, inducing a much faster, stronger, and broader resistance in the whole plant, termed systemic acquired resistance (SAR), in response to a secondary infection by a wide variety of pathogens (Fu and Dong, 2013).

Studies have shown that the plant hormone salicylic acid (SA) is required for both local defense and SAR against biotrophic and semi-biotrophic pathogens (Fu and Dong, 2013). *Arabidopsis* mutants that are defective in SA biosynthesis or accumulation, such as *ics1*, *eds1*, *pad4*, and *eds5* mutants, show



¹Institute of Plant Protection, Jiangsu Academy of Agricultural Sciences, Nanjing, Jiangsu 210014, P. R. China

²Department of Biological Sciences, University of South Carolina, Columbia, SC 29208, USA

³Department of Plant Pathology, Nanjing Agricultural University, Nanjing, Jiangsu 210095, P. R. China

⁴Center for Plant Science Innovation and the Department of Plant Pathology, University of Nebraska, Lincoln, NE 68588, USA

⁵Department of Biochemistry and Molecular Biology, Colorado State University, Fort Collins, CO 80526, USA

⁶Lead Contact

^{*}Correspondence: fqliu20011@sina.com (F.L.), zfu@mailbox.sc.edu (Z.Q.F.) https://doi.org/10.1016/j.chom.2017.10.019

enhanced susceptibility to pathogen infection and are defective in SAR (Lu, 2009). Exogenous application of SA will dramatically induce the expression of antimicrobial PR proteins and increase disease resistance (Shah et al., 1997). A gene called NPR1 (NON-EXPRESSER OF PR GENES 1) was identified through genetic screens for Arabidopsis mutants that are defective in inducing PR gene expression (Cao et al., 1994). Furthermore, npr1 mutants display increased disease susceptibility to bacterial and fungal pathogens, indicative of NPR1's indispensable roles in plant defense. NPR1 protein is predominantly localized in the cytosol as oligomers in non-induced conditions. Induction of SA by pathogen attack reduces the oligomeric NPR1 into monomers through association with thioredoxins, allowing NPR1 monomers to enter the nucleus (Kinkema et al., 2000; Mou et al., 2003; Tada et al., 2008). As transcriptional coactivators. NPR1 monomers interact with TGA transcription factors, which bind the promoter of PR genes, to activate the expression of PR genes (Fu and Dong, 2013). NPR1 modulates expression of a large set of genes (2,248), corresponding to almost 99% of SA-responsive genes, highlighting the importance of NPR1 in SA signaling pathways and in transcriptional reprogramming during plant defense (Wang et al., 2006). Currently, only a few plant pathogen effectors have been reported to influence SA-regulated plant defense (Tanaka et al., 2015). For example, P. syringae Hopl1 recruits Hsp70 into chloroplasts and presumably causes chloroplast remodeling to suppress SA biosynthesis or transport (Jelenska et al., 2007). SA is synthesized through the ICS1 (isochorismate synthesis 1) pathway during pathogen infection in Arabidopsis plants (Wildermuth et al., 2001). ICS1 converts chorismate into isochorismate and then presumably an unidentified IPL (isochorismate pyruvate lyase) converts isochorismate into SA (Chen et al., 2009). More recently, the fungal chorismate mutase, Cmu1, and two isochorismatases, the oomycete PsLsc1 and the fungal VdLsc1, were shown to affect SA biosynthesis (Diamei et al., 2011; Liu et al., 2014). In addition to targeting SA biosynthesis, some pathogen effectors target SA signaling via various mechanisms. P. syringae HopM1/AvrE effectors suppress SA-dependent basal immunity (DebRoy et al., 2004) and a nuclear localized downy mildew effector HaRxL44 mediated the degradation of Mediator subunit 19a to attenuate SA-mediated plant defense (Caillaud et al., 2013).

Since NPR1 functions as a master regulator of plant defense and SA signaling, we speculated that type III effectors from P. syringae would directly target NPR1 to disrupt plant immunity. To test this hypothesis, a conventional yeast two-hybrid (Y2H) screen was deployed to identify potential pathogen effectors that bind NPR1. Here, we show that SA facilitates the interaction between the P. syringae type III effector AvrPtoB and NPR1. AvrPtoB mediates the degradation of NPR1 dependent on its E3 ligase activity, through the host 26S proteasome in the presence of SA, which contributes to pathogen virulence and inhibition of plant defense. Furthermore, we demonstrate that NPR1 is a positive regulator of MTI and show that different classes of NPR1-dependent SA signaling genes are suppressed by AvrPtoB during immune responses. Thus, we propose a model in which AvrPtoB targets SA-stimulated, functional NPR1, and impairs SA-dependent transcriptional reprogramming to suppress host immunity.

RESULTS

SA Facilitates AvrPtoB-NPR1 Interaction in Y2H Assays

To test our hypothesis regarding the targeting of NPR1 by pathogen effectors, we used a Y2H assay to investigate the physical interactions between P. syringae type III effectors and NPR1 (Baltrus et al., 2011; Mukhtar et al., 2011). Among the effectors identified through these screens, AvrPtoB was found to interact with NPR1 weakly in the absence of SA (Figure 1A). Interestingly, addition of SA dramatically enhanced its interaction with NPR1. Moreover, two active analogs of SA, 3,5-dichlorosalycilic acid (DCSA) and 2,6-Dichloroisonicotinic acid (INA), also strongly promoted the interaction between AvrPtoB and NPR1. By contrast, the SA inactive analog 3-hydroxy benzoic acid (3HBA) showed no effect on this interaction. To show that this interaction is specific, we compared the interaction between NPR1 and AvrPtoB with the interaction between NPR1 and AvrPto. Although sequence unrelated, both AvrPto and AvrPtoB can interact with Pto kinase and activate ETI via the coil-coiled NBS-LRR type R protein Prf (Salmeron et al., 1996; Kim et al., 2002). As shown in Figure S1D, AvrPto showed no interaction with NPR1 in the presence of SA. These data indicate that the SA-dependent interaction between AvrPtoB and NPR1 is specific.

Distinct Regions of AvrPtoB and NPR1 Are Required for Y2H Interaction

AvrPtoB contains an N-terminal Pto-interacting domain (PID) between amino acids 121 and 200 (Xiao et al., 2007) and a C-terminal U-box type E3 ubiquitin ligase domain (Figure S1A). The amino acid residues 1-387 of AvrPtoB are necessary and sufficient for interacting with BAK1 and Fen kinases (Shan et al., 2008; Cheng et al., 2011; Mathieu et al., 2014); however, a shorter N-terminal region, AvrPtoB₁₋₃₀₇, is responsible for its interaction with CERK1, Bti9, and MKK2 (Gimenez-Ibanez et al., 2009; Zeng et al., 2012; Wei et al., 2015). To identify specific domains in AvrPtoB that interact with NPR1, we generated a series of AvrPtoB truncations and point mutations and conducted Y2H assays in the presence of SA (Figures S1A and S1B). Two deletion mutants, AvrPtoB₁₋₃₀₇ and AvrPtoB₁₋₃₈₇, and AvrPtoB_{E3-LOF} (an inactive E3 ligase form containing point mutations in three E2 enzyme binding sites: F479A/F525A/P533A; Mathieu et al., 2014) showed significant interaction with NPR1 in the presence of SA (Figures 1B and S1B), suggesting that residues 1-307 are sufficient for AvrPtoB's interaction with NPR1 and that its E3 ligase domain is dispensable for the interaction. Additional truncated constructs AvrPtoB₁₋₂₀₅, AvrPtoB₃₀₈₋₄₃₆, and AvrPtoB₃₀₈₋₅₅₃ exhibited no detectable interaction with NPR1 (Figures 1B and S1B). Thus, AvrPtoB₂₀₆₋₃₀₇, just behind the PID, is necessary for specific interaction between AvrPtoB and NPR1 in the presence of SA, which is distinct from AvrPtoB's interacting regions with Pto, BAK1, and Fen (Wirthmueller et al., 2013).

NPR1 protein consists of an ankyrin repeat (AKR) in the central region (Cao et al., 1997), an N-terminal broad complex, tram track, bric-à-brac/poxvirus and zinc-finger (BTB/POZ) domain, and a putative transcriptional activation domain with acidic amino acids in the C-terminal region (Figure S1C). To further characterize critical motifs required for NPR1-AvrPtoB interaction, various mutagenesis approaches along with certain NPR1

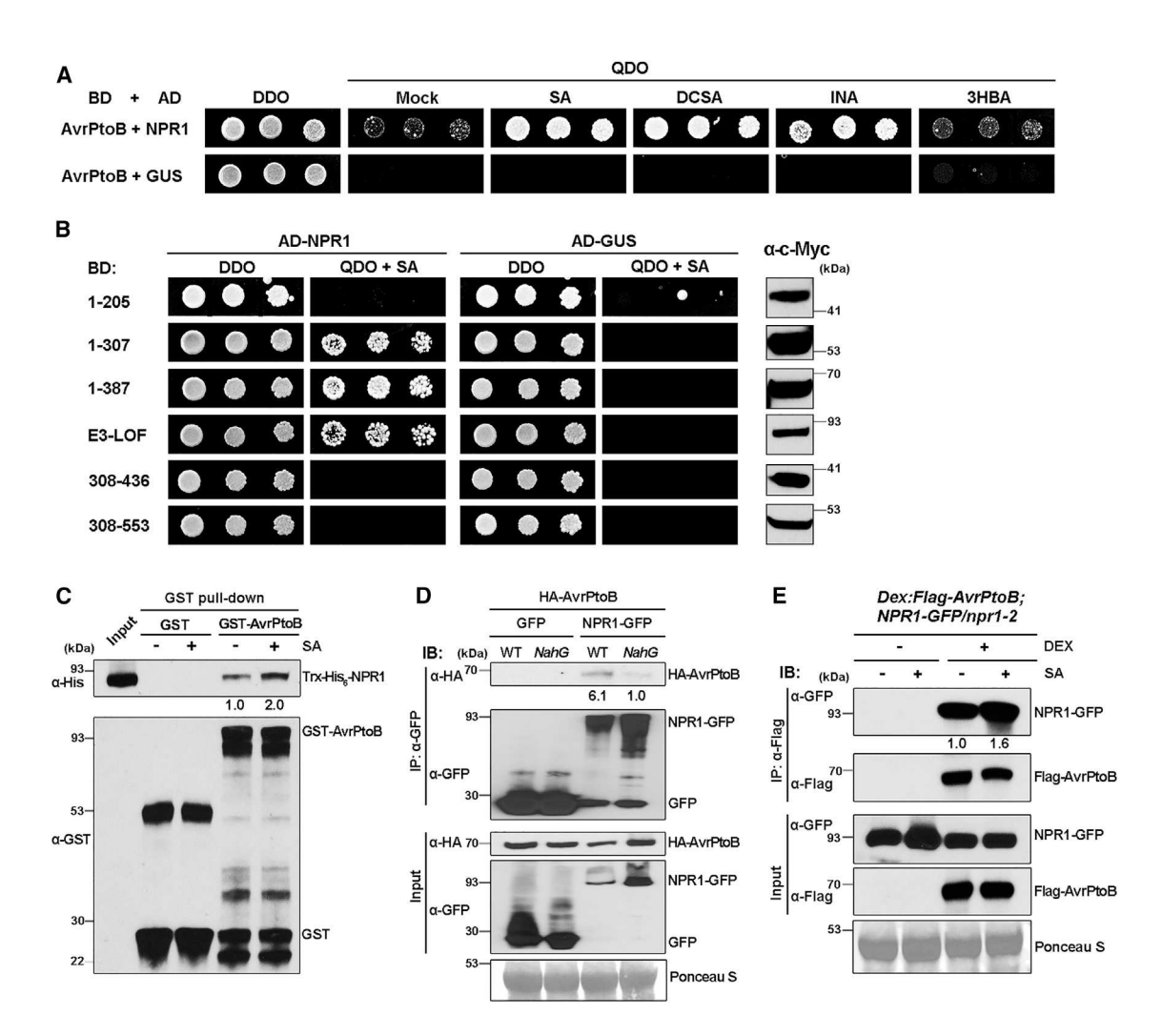


Figure 1. SA Promotes AvrPtoB Interaction with NPR1

(A) SA and its active analogs facilitate interaction between NPR1 and AvrPtoB in Y2H assays. Yeast diploids selected on double synthetic dropout (DDO) medium lacking histidine and tryptophan were tested for growth on selective quadruple dropout (QDO) medium lacking tryptophan, leucine, adenine, and histidine. SA (0.2 mM), its active analogs DCSA, INA, or the inactive analog 3-HBA was supplemented in QDO medium. Colony growth was scanned after 3 days of incubation. (B) AvrPtoB₁₋₃₀₇ is necessary for interaction with NPR1 in Y2H assays. Yeast cells grown on DDO and selective QDO media supplemented with 0.2 mM SA are shown. Expression of various AvrPtoB deletion constructs in yeast was detected by immunoblot using α -c-Myc antibodies (right). E3-LOF, AvrPtoB_{E3-LOF}. (C) In vitro pull-down assays of Trx-His₆-NPR1 with GST-AvrPtoB fusion protein. The precipitation of Trx-His₆-NPR1 protein with GST-AvrPtoB bound glutathione particles was detected by immunoblot using α -His antibody before (input) and after washes (pull-down). The same eluted protein was also blotted with α -GST antibody to show approximately equal amount of recombinant protein. The signal intensities of precipitated Trx-His₆-NPR1 protein by application of SA (+) or not (-) were quantified and normalized to the intensity of the corresponding GST-AvrPtoB proteins. Relative Trx-His₆-NPR1 band intensity is quantified below (normalized to GST-AvrPtoB and relative to control).

(D) Co-immunoprecipitation (coIP) of AvrPtoB with NPR1 in *N. benthamiana*. HA-AvrPtoB and NPR1-GFP under control of the cauliflower mosaic virus 35S promoter were transiently co-expressed in wild-type (WT) or *NahG* transgenic *N. benthamiana* leaves by agroinfiltration. Protein extracts collected after 50 μM MG115 treatment were subjected to coIP. The immunoprecipitated (IP) and input proteins were analyzed via immunoblot (IB) assay using α-HA and α-GFP antibodies. The signal intensities of co-immunoprecipitated HA-AvrPtoB proteins were quantified and normalized to that in the input fractions. Relative HA-AvrPtoB band intensity is shown below (normalized to precipitated NPR1-GFP and relative to *NahG* plants).

(E) CoIP of NPR1 with AvrPtoB in transgenic Arabidopsis. T_3 transgenic Arabidopsis expressing the Flag-AvrPtoB under control of a Dex-inducible promoter in the 35S:NPR1-GFP/npr1-2 background (Dex:Flag-AvrPtoB; NPR1-GFP/npr1-2) was used. Five-week-old soil-grown plants were treated with 3 μ M DEX and/or 0.5 mM SA for 12 hr. Leaf extracts were immunoprecipitated (IP) with α -Flag beads and eluted proteins were analyzed by IB with α -GFP and α -Flag antibodies. Relative NPR1-GFP band intensity is denoted below (normalized to immunoprecipitated Flag-AvrPtoB and relative to control).

Ponceau S staining of Rubisco large subunit was used to monitor equal loading of total proteins. Numbers on the left axis represent the molecular mass size of marker in kilodaltons (kDa).

See also Figure S1.

deletion mutants were utilized in Y2H assays with and without the addition of SA (Figures S1D and S1E). Among these mutants, the NPR1 $_{1-280}$ fragment containing only the BTB/POZ domain

did not show interaction with AvrPtoB, whereas C-terminal NPR1₁₅₀₋₅₉₃ including the AKR motif was sufficient for the interaction (Figure S1D). Moreover, several point mutants, such as

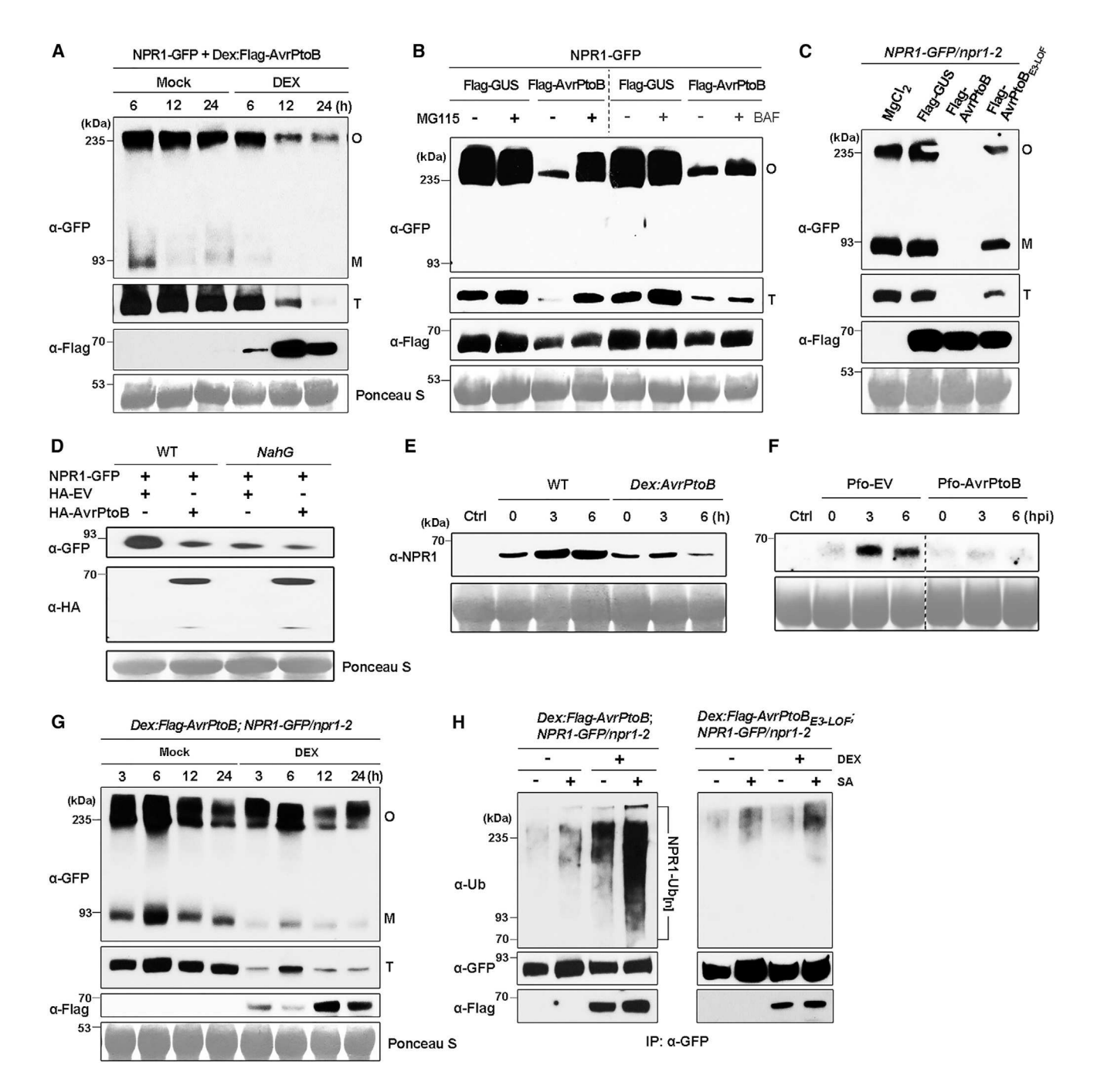


Figure 2. AvrPtoB Mediates NPR1 Degradation by 26S Proteasome

(A) Inducible expression of AvrPtoB triggers NPR1 degradation. Dex:Flag-AvrPtoB was co-expressed with 35S:NPR1-GFP in N. benthamiana by agroinfiltration and leaf extracts were obtained after mock or DEX treatment at indicated times.

- (B) The proteasome inhibitor MG115 blocks AvrPtoB-triggered NPR1 degradation. 35S:NPR1-GFP transiently co-expressed with 35S:Flag-AvrPtoB or 35S:Flag-GUS in N. benthamiana and leaf extracts were isolated after treatment with 100 µM MG115 or 300 nM Bafilomycin A1 (BAF).
- (C) AvrPtoB mediates NPR1 degradation in an E3 ligase-dependent manner. 35S:Flag-GUS, 35S:Flag-AvrPtoB and 35S:Flag-AvrPtoB_{E3-LOF} were transiently expressed by Agrobacterium in 35S:NPR1-GFP/npr1-2 transgenic Arabidopsis, respectively.
- (D) SA facilitates NPR1 destabilization mediated by AvrPtoB. 35S:HA-AvrPtoB and 35S:NPR1-GFP were co-expressed in wild-type or NahG transgenic N. benthamiana by agroinfiltration. HA fused with empty vector (EV) under the 35S promoter was used as a negative control.
- (E) Inducible expression of AvrPtoB causes a reduction of endogenous NPR1 level. The WT and Nd/Dex:AvrPtoB transgenic Arabidopsis were treated with 0.5 mM SA for 12 hr and then sprayed with 3 µM DEX by indicated time points. The plant untreated with SA was utilized as a control (Ctrl).
- (F) Pfo-AvrPtoB promotes native NPR1 degradation in response to SA. WT Arabidopsis leaves were treated with 0.5 mM SA for 6 hr and then infiltrated with Pfo carrying the EV or AvrPtoB by indicated hr post inoculation (hpi).

npr1-1, npr1-5, and nim1-2 in the AKR domain, and an additional AKR deletion mutant (ΔAKR) all lost their ability to interact with AvrPtoB in the presence of SA (Figure S1D). These results indicate that the AKR domain of NPR1 is required for its interaction with AvrPtoB.

AvrPtoB Interaction with NPR1 Is Enhanced by SA In Vitro and In Vivo

To test if SA promotes the direct interaction between AvrPtoB and NPR1, we carried out pull-down assays in the presence and absence of SA using purified recombinant glutathione-Stransferase (GST)-tagged AvrPtoB and thioredoxin (Trx)-His₆tagged NPR1 fusion proteins expressed in Escherichia coli. The purified GST-AvrPtoB protein was immobilized on glutathione Sepharose beads and mixed and incubated with cell lysates containing the Trx-His₆-NPR1 fusion protein. After washing, the Trx-His₆-NPR1 protein was efficiently pulled down by GST-AvrPtoB (Figure 1C). Addition of SA increased the amount of Trx-His₆-NPR1 protein pulled down by GST-AvrPtoB. In contrast, equivalent amounts of GST protein alone did not bind to Trx-His₆-NPR1 under any condition. Apparently, AvrPtoB can directly bind to NPR1 and exogenous SA significantly increased their binding affinity in vitro.

To investigate the association of AvrPtoB and NPR1 in planta, we performed co-immunoprecipitation (coIP) assays in Nicotiana benthamiana and transgenic Arabidopsis. First, AvrPtoB protein with an N-terminal HA-tag (HA-AvrPtoB) and NPR1 protein with a C-terminal GFP tag (NPR1-GFP) were transiently coexpressed in N. benthamiana by infiltration with Agrobacterium tumefaciens. The HA-AvrPtoB proteins were effectively coimmunoprecipitated by NPR1-GFP covalently bound to beads (Figure 1D), indicating that AvrPtoB is associated with NPR1 in planta. The NahG gene isolated from the soil bacterium Pseudomonas putida encodes a salicylate hydroxylase, which degrades SA into SAR-inactive catechol (Delaney et al., 1994). In NahG transgenic N. benthamiana, HA-AvrPtoB protein was not found to be efficiently associated with NPR1-GFP protein (Figure 1D). These results indicate that endogenous SA enhances NPR1 binding to AvrPtoB in N. benthamiana.

Next, we carried out reciprocal coIP experiments to investigate the interaction between NPR1 and AvrPtoB in Arabidopsis. T₃ transgenic Arabidopsis expressing Flag-AvrPtoB under the control of a dexamethasone (DEX)-inducible promoter in the NPR1-GFP/npr1-2 background were generated. Figure 1E shows that NPR1-GFP protein was sufficiently co-immunoprecipitated with the conjugated beads in DEX-treated transgenic Arabidopsis expressing Flag-AvrPtoB but not in mock-treated plants. Besides, NPR1-GFP could be recruited by Flag-AvrPtoB with a slightly higher affinity compared with that without SA treatment (Figure 1E). These results clearly illustrate that SA facilitates the association between NPR1 and AvrPtoB in Arabidopsis.

SA Promotes AvrPtoB-Mediated Degradation of NPR1

Since AvrPtoB functions as an active U-box E3 ligase and mediates degradation of membrane RLKs (e.g., FLS2 and CERK1) in the cytoplasm (Gohre et al., 2008; Gimenez-Ibanez et al., 2009), we next examined whether the stability of NPR1 is affected by AvrPtoB in planta. We observed that NPR1-GFP protein was significantly lower in N. benthamiana leaves co-expressing DEX-inducible Flag-AvrPtoB and NPR1-GFP after 12 hr of DEX treatment compared with total extracts without DEX treatment (Figure 2A). DEX treatment did not affect the expression and transcription of NPR1-GFP (Figure S2A). Also, leaves co-expressing Flag-AvrPtoB and NPR1-GFP exhibited a significantly lower level of NPR1-GFP protein compared with leaves co-expressing Flag-GUS and NPR1-GFP (Figure 2B). These findings indicate that AvrPtoB causes the degradation of NPR1 in N. benthamiana.

To identify the primary NPR1 degradation pathway, a 26S proteasome inhibitor, MG115, and a selective inhibitor of vacuolartype H⁺-ATPase, Bafilomycin A1 (BAF), were employed to block specific protein degradation pathways in plants. As shown in Figure 2B, only MG115 significantly blocked AvrPtoB-mediated NPR1 destabilization, suggesting that NPR1 undergoes degradation by the 26S proteasome rather than through vacuoles. In addition, we found that the E3 ligase catalytically inactive mutant AvrPtoB_{E3-LOF} was compromised in its ability to degrade NPR1 by agroinfiltration in NPR1-GFP/npr1-2 transgenic Arabidopsis (Figure 2C). This result was consistent with our data obtained using non-pathogenic Pseudomonas fluorescens 55 (Pfo) to deliver AvrPtoB or AvrPtoB_{E3-LOF} into *Arabidopsis* and by co-expressing AvrPtoB or AvrPtoB_{E3-LOF} with NPR1-GFP in N. benthamiana (Figures S2B and S2C). Collectively, these data indicate that AvrPtoB triggers NPR1 degradation via the 26S proteasome pathway in an E3 ligase-dependent manner.

To further substantiate the role of SA in AvrPtoB-mediated NPR1 degradation, we transiently expressed the aforementioned constructs in NahG transgenic N. benthamiana. Clearly, the AvrPtoB-mediated NPR1 degradation was more pronounced in wild-type plants than in NahG transgenic plants (Figure 2D), indicating that there was less NPR1 protein in NahG plants, and endogenous SA in wild-type plants could facilitate AvrPtoB-mediated NPR1 degradation in N. benthamiana. Next, we focused on investigating the regulation of endogenous NPR1 stability by AvrPtoB in Arabidopsis. It has been reported that the basal NPR1 protein level is very low due to constitutive elimination by proteolysis (Tada et al., 2008; Spoel et al.,

(G) Inducible expression of AvrPtoB triggers NPR1-GFP degradation by SA. The Dex:Flag-AvrPtoB;NPR1-GFP/npr1-2 #3 transgenic Arabidopsis was treated with 0.5 mM SA for 12 hr and then infiltrated with buffer (mock) or 1 μ M DEX by indicated times.

(H) AvrPtoB-mediated in vivo poly-ubiquitination of NPR1. Leaves of Dex:Flaq-AvrPtoB;NPR1-GFP/npr1-2 #3 or Dex:Flaq-AvrPtoB_{E3-1 OF}:NPR1-GFP/npr1-2 #16 transgenic Arabidopsis incubated with 100 µM MG115 were infiltrated either with 1 µM Dex and/or 0.2 mM SA or mock for 12 hr. Protein extracts were immunoprecipitated (IP) with α-GFP beads. The bound proteins and input were subjected to reducing SDS-PAGE and analyzed by immunoblotting using α-Ubiquitin (Ub), α-GFP, and α-Flag antibodies. Poly-ubiquitinated forms of NPR1 (NPR1-Ub_[n]) were detected as high-molecular-weight smears.

NPR1-GFP proteins were separated by non-reducing and reducing SDS-PAGE gel followed by immunoblot using α -GFP and α -Flag antibodies. NPR1-GFP oligomeric (O), monomeric (M), and total (T) proteins were detected. See also Figure S2.

2009). SA significantly increases NPR1 protein level and can concomitantly lead to degradation by Cullin 3 E3 ligase, mediated by NPR3 and NPR4 as adaptors in the nucleus to maintain the optimum NPR1 protein level (Tada et al., 2008; Spoel et al., 2009; Fu et al., 2012). To determine whether AvrPtoB destabilizes the endogenous NPR1 protein in the presence of SA, we treated the wild-type and the inducible AvrPtoB transgenic Arabidopsis with DEX, followed by SA application or a combination of SA and DEX treatment. We found a reduced NPR1 protein level in the transgenic line (Figures 2E and S2D). Similarly, AvrPtoB delivered alone by Pfo 55 (Guo et al., 2009), which carries a cosmid containing the type III secretion apparatus of P. syringae, could also robustly inhibit the accumulation of NPR1 after the SA treatment (Figure 2F). These results reveal that AvrPtoB facilitates endogenous NPR1 degradation in Arabidopsis. In addition, NPR1-GFP, especially the monomeric form, was shown to be significantly decreased upon induction of AvrPtoB in transgenic Arabidopsis after exogenous SA application (Figure 2G) and NPR1-GFP protein was not affected by DEX treatment (Figure S2E), supporting that AvrPtoB promotes NPR1 degradation in response to SA.

Since AvrPtoB directly interacts with NPR1 and mediates NPR1 degradation dependent on its E3 ligase activity, we determined if AvrPtoB promotes NPR1 poly-ubiquitination. As shown in Figure 2H, immune-precipitated NPR1-GFP was highly poly-ubiquitinated in DEX-inducible *AvrPtoB* but not in *AvrPtoB*_{E3-LOF} transgenic *Arabidopsis*, and the poly-ubiquitination of NPR1-GFP was significantly enhanced by SA. Collectively, these results demonstrate that AvrPtoB promotes the poly-ubiquitination and subsequent degradation of NPR1 in the presence of SA via the host 26S proteasome dependent on its E3 ligase activity *in planta*.

AvrPtoB Suppresses NPR1-Mediated Plant Defense

To assess whether degradation of NPR1 is important for AvrPtoB-mediated promotion of P. $syringae\ pv$. $tomato\ (Pst)$ DC3000 pathogenicity in Arabidopsis, we analyzed bacterial multiplication of DC3000 and DC3000 $\Delta avrPtoB$ mutant (a DC3000 mutant lacking AvrPtoB) in Arabidopsis. In Col-0 plants, the growth of $\Delta avrPtoB$ mutant was significantly reduced compared with DC3000 (Figure 3A), supporting the strong virulence activity of AvrPtoB on Arabidopsis. In npr1-2 mutant plants, however, both strains showed increased bacterial multiplication and enhanced disease symptoms (Figures 3A and S3A). There was no significant difference between the growth of DC3000 and the growth of $\Delta avrPtoB$ in npr1-2 plants when they were infiltrated into npr1-2. These data demonstrate that the virulence function of AvrPtoB is dependent on NPR1. Therefore, NPR1 is the major virulence target of AvrPtoB.

We next studied whether AvrPtoB delivered into plant cells by the DC3000 type III secretion system affects native NPR1 protein in *Arabidopsis*. Wild-type DC3000 and the DC3000 $\Delta avrPtoB$ mutant were infiltrated into *Arabidopsis* Col-0 plants. We detected a significantly higher level of NPR1 protein in *Arabidopsis* upon $\Delta avrPtoB$ mutant infection compared with that by DC3000 inoculation, indicating that AvrPtoB plays an important role in the degradation of native NPR1 protein during DC3000 infection (Figure 3B). In particular, this finding implies that NPR1 already induces long-lasting but weaker MTI before being shut down

by AvrPtoB. Consistently, the expression of PR1 protein, which is controlled by NPR1, is significantly reduced in DC3000-infiltrated Arabidopsis leaf samples compared with ΔavrPtoB-infiltrated samples (Figure 3B). Intriguingly, the possible slight induction of NPR1 transcription by \(\Delta avrPtoB \) is lower than that by DC3000 (Figures S3B and S3C), demonstrating that AvrPtoB destabilizes NPR1 by post-transcriptional regulation. Moreover, the NPR1-GFP protein level in transgenic Arabidopsis was dramatically decreased after infection by DC3000, but not when the plants were challenged with ΔavrPtoB, DC3000 hrcC mutant (a type III secretion-defective mutant that is deficient in delivering effectors into host cells), or the double mutant strain DC3000 ΔavrPtoBΔavrPto (Figures 3C and S4). The degradation of NPR1-GFP protein by DC3000 was also accompanied by a decreased nuclear NPR1-GFP protein level as visualized by fluorescence in Arabidopsis leaves (Figure 3D). Thus, AvrPtoB destabilizes NPR1 protein by post-transcriptional regulation after bacterial infection in Arabidopsis.

DC3000 \(\textit{\Delta} \text{vPtoB} \) Mutants Elicit Elevated NPR1-Regulated Cell-Wall-Associated Plant Defense

Previous studies have demonstrated that a subset of type III effectors, including AvrPtoB, can suppress callose deposition triggered by MAMPs (de Torres et al., 2006; Guo et al., 2009). To further characterize the nature of cell-wall-based immunity impaired by AvrPtoB, we employed the DC3000 ΔavrPtoB mutant strain to examine cell-wall callose papillae formation. Strikingly, the \(\Delta avrPtoB \) mutant elicited a higher level of callose papillae in wild-type Arabidopsis compared with DC3000 (Figure 4A). Next, to evaluate the requirement of NPR1 for ΔavrPtoB-enhanced cell-wall deposition, we determined the amount of callose deposition by cytological examination in leaves of npr1-2 mutant Arabidopsis infected by DC3000 or ΔavrPtoB strain. The ability to mount the cell-wall-associated plant defense elicited by \(\Delta avrPtoB \) in wild-type plants was significantly reduced in npr1-2 plants (Figure 4A). This result correlates with the increased susceptibility of npr1-2 plants to ΔavrPtoB (Figure 3A). Therefore, the △avrPtoB mutant is compromised in its virulence and shows elevated NPR1-dependent cell-wall defense, supporting the hypothesis that AvrPtoB is capable of repressing NPR1-mediated basal immunity.

It has been shown that two callose synthase genes, also referred to as glucan synthase-like genes GSL5 and GSL6, are involved in the NPR1-dependent SA signaling pathway (Dong et al., 2008). To better understand the signal transduction pathways leading to callose deposition induced by pathogens, we further analyzed the expression of these callose synthase genes in Col-0 and npr1-2 plants in response to DC3000 or ΔavrPtoB mutant. Although both GSL5 and GSL6 genes were significantly activated in response to pathogen attacks (Figure 4B), the induction of the expression of these genes was more pronounced in ΔavrPtoB mutant infiltrated Col-0 plants. Moreover, the expression of these two genes was significantly compromised in npr1-2 plants. We also used PR1 expression as a marker of SA signaling. A high level of PR1 transcripts was observed in Col-0 but not in npr1-2 plants, consistent with increased accumulation of PR1 protein in Col-0 by ΔavrPtoB mutant infection (Figure 4B). Therefore, AvrPtoB represses NPR1-mediated SA signaling genes to inhibit plant immune responses.

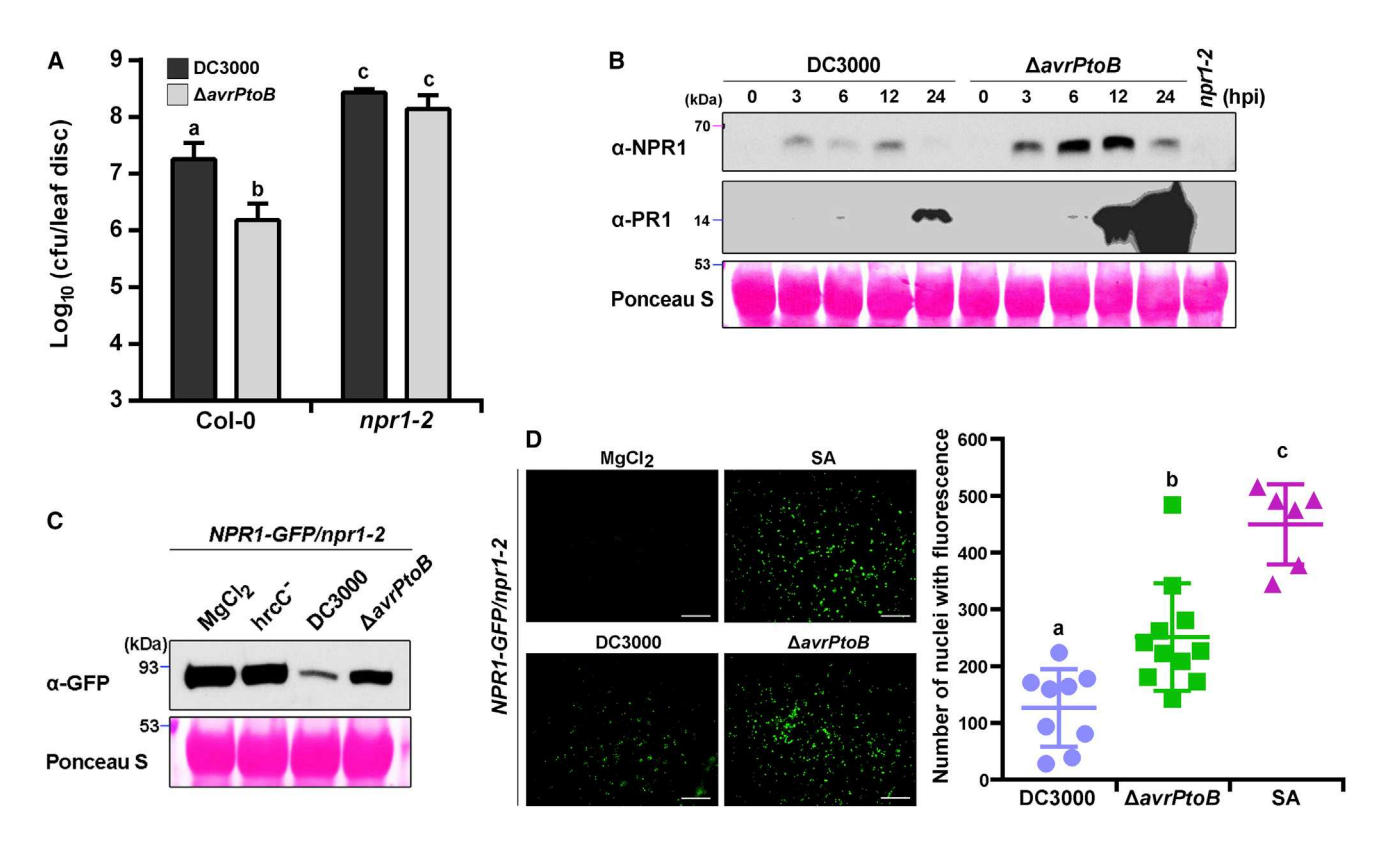


Figure 3. AvrPtoB Overcomes NPR1-Mediated Defense

(A) The type III effector AvrPtoB promotes P. syringae multiplication on Arabidopsis dependent on its ability to disable NPR1 function. Bacterial growth of Pst DC3000 and $\Delta avrPtoB$ mutant was measured 3 days post infiltration with bacteria at 10^6 cfu/mL in Arabidopsis Col-0 or npr1-2 plants. Error bars represent SD. Different letters indicate the statistical significance (two-way ANOVA, Tukey's test; $\alpha = 0.05$, n = 8). cfu, colony-forming units.

(B) Loss of AvrPtoB effector in DC3000 (Δ avrPtoB) enhances the expression of endogenous NPR1 and PR1 proteins. The soil-grown leaves of wild-type Col-0 *Arabidopsis* were hand infiltrated with DC3000 or Δ avrPtoB mutant at 10⁸ cfu/mL and harvested at different hpi. The total endogenous NPR1 and PR1 proteins were analyzed by immunoblotting with α -NPR1 and α -PR1 antibodies, respectively.

(C) DC3000 triggers NPR1-GFP degradation. The 35S:NPR1-GFP/npr1-2 transgenic Arabidopsis seedlings were incubated with MgCl₂ or indicated bacteria at OD₆₀₀ = 0.6 for 12 hr. Immunoblot analysis of total NPR1-GFP protein was performed using α -GFP antibody.

(D) DC3000 infection reduces nuclear import of NPR1-GFP in local leaves. The soil-grown leaves of 35S:NPR1-GFP/npr1-2 transgenic Arabidopsis were infiltrated with MgCl₂, 0.2 mM SA or bacterial with 10^8 cfu/mL for 12 hr. GFP signals were visualized by fluorescence microscopy (left). Scale bar, $100 \mu m$. Quantitative analysis of the number of nuclei with GFP fluorescence is shown (right). Error bars indicate \pm SD. Different letters indicate the statistical significance (one-way ANOVA, Sidak's test; $\alpha = 0.05$, n = 9).

Experiments in all panels were repeated two to three times with similar results. See also Figures S3 and S4.

Transgenic Expression of *AvrPtoB* Restores the Virulence of *∆avrPtoB* and Suppresses MTI and SA-Mediated Plant Immunity

We have established that AvrPtoB promotes DC3000 pathogenicity by destabilizing NPR1 protein. Using inducible *AvrPtoB* transgenic *Arabidopsis* plants, we determined whether AvrPtoB expressed in host leaf cells could restore the virulence of the DC3000 Δ*avrPtoB* mutant. Transgenic expression of *AvrPtoB* almost fully complemented the virulence defect of the Δ*avrPtoB* mutant, allowing the Δ*avrPtoB* mutant to multiply to a population level similar to wild-type DC3000 (Figures 5A, S5A, and S5B). In contrast, the *AvrPtoB_{E3-LOF}* lines did not recover the virulence of the Δ*avrPtoB* mutant, indicating that the E3 ligase activity of AvrPtoB plays an important role in the pathogenesis of DC3000 in *Arabidopsis*.

It is well known that the DC3000 *hrcC*⁻ mutant is potent in activating MTI (Hauck et al., 2003). To investigate if transgenic expression of *AvrPtoB* in *Arabidopsis* suppresses MTI, we first

evaluated the ability of AvrPtoB and AvrPtoB_{E3-LOF} transgenic lines to mount a defense response induced by the *hrcC*⁻ strain. In AvrPtoB transgenic lines, the growth of hrcC- was dramatically enhanced when compared with Col-0 wild-type Arabidopsis (Figures 5B and S5B). Notably, this enhanced multiplication was partially dependent on an intact AvrPtoB E3 ligase catalytic site, as multiplication of *hrcC*⁻ in *AvrPtoB_{E3-LOF}* transgenic lines only slightly increased in comparison with Col-0 plants. Pretreatment of Arabidopsis leaves with the flg22 peptide, a 22-amino acid flagellin peptide known to activate MTI, prior to infection with virulent pathogen P. syringae has been demonstrated to reduce susceptibility to this pathogen (Gomez-Gomez et al., 1999). We then investigated flg22-triggered disease resistance in Col-0, AvrPtoB, and AvrPtoB_{E3-LOF} transgenic Arabidopsis. As expected, flg22-induced MTI is compromised in AvrPtoB transgenic plants compared with Col-0 (Figures 5C and S5B). In contrast, flg22-induced resistance against DC3000 is not suppressed in the $AvrPtoB_{E3-LOF}$ lines. Overall, the inducible

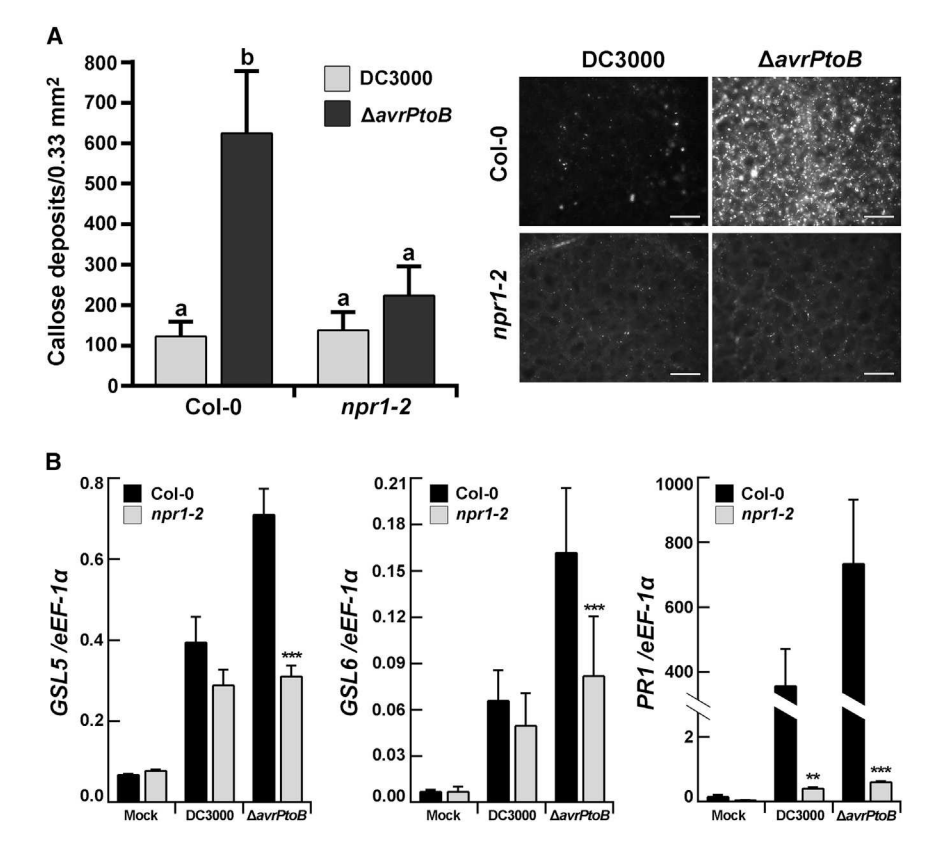


Figure 4. AvrPtoB Suppresses NPR1-Dependent Cell-Wall-Based Defense

(A) Loss of AvrPtoB (Δ avrPtoB mutant) enhances NPR1-mediated callose deposition. Leaves of soilgrown Col-0 and npr1-2 Arabidopsis were infected by indicated pathogens for 12 hr at 10^8 cfu/mL and then subjected to staining. The stained leaves were imaged by fluorescence microscopy using the same settings. The number of callose foci was quantified by ImageJ (left). Error bars represent SD. Different letters indicate the statistical significance (two-way ANOVA, Tukey's test; α = 0.05, n = 10). Representative images from two independent experiments are displayed (right). Scale bar, 100 µm.

(B) $\Delta avrPtoB$ mutant induces higher expression of NPR1-dependent defense genes. Total RNA was extracted from leaves at 16 hpi. Expression of GSL5, GSL6, and PR1 was analyzed by qRT-PCR. Relative expression levels were normalized to the reference gene $eEF-1\alpha$. Error bars represent SD. Asterisks indicate significant differences between Col-0 and npr1-2 (multiple t tests, one per row, **p < 0.01, ***p < 0.001; n = 4).

MAMP signaling. NPR1 protein is strongly upregulated by DC3000 *hrcC*⁻ mutant or flg22 treatment (Figure 6A), although foliar infiltration of DC3000 *hrcC*⁻ resulted in a moderate induction of *NPR1* transcripts in Col-0 *Arabidopsis* (Figure S6C). NPR1

induction was nearly eliminated in the SA accumulation mutants (eds1, pad4, ics1, and eds5) (Figure S6A), revealing that NPR1 protein accumulation is regulated in an SA-dependent manner during MAMP signaling (Fu et al., 2012).

To investigate the importance of NPR1 in MTI, we evaluated the contribution of NPR1 to callose deposition and marker gene expression in MAMP signaling. As demonstrated in Figure 6B, NPR1 positively regulates cell-wall-associated plant defense in response to the DC3000 hrcC-. Conversely, flg22elicited callose deposition was not compromised in npr1-2 (Figure S6B). To further analyze the expression of a later response gene (PR1) and early defense marker genes, including FRK1, AT2G17740, WRKY6, and WRKY29 in MAMP signaling, the induction kinetics of these genes were monitored in Col-0 and npr1-2 after hrcC challenge. PR1 expression in response to hrcC⁻ was strongly reduced in npr1-2 (Figure S6C). In addition, activation of the early MAMP marker genes was also significantly impaired in npr1-2 mutant after pathogen challenge (Figure S6C). These results indicate that NPR1 functions as a potent regulator to positively regulate multiple MAMP signaling responses.

expression of *AvrPtoB in planta* blocks MTI activated by *hrcC*⁻ or flg22 in a manner dependent on its E3 ligase activity.

NPR1 was reported to play a vital role in SA signal transduction and SAR. Based on our prior observations in *Arabidopsis*, AvrPtoB can degrade native NPR1 protein, implying that AvrPtoB could impede SA-mediated plant immunity and SAR. Foliar pretreatment with SA resulted in an enhanced resistance to subsequent infection by a virulent pathogen, *P. syringae pv.* maculicola (*Psm*) ES4326, in wild-type Col-0 *Arabidopsis* (Figures 5D and S5C). Like *npr1-2* mutant plants, SA-induced plant defense was strongly impaired in *AvrPtoB* transgenic *Arabidopsis* but not in *AvrPtoBe3-LOF* transgenic plants. This finding further supports that expression of *AvrPtoB* in plants inhibits SA-regulated plant immunity and that the E3 ligase activity is required for this inhibition.

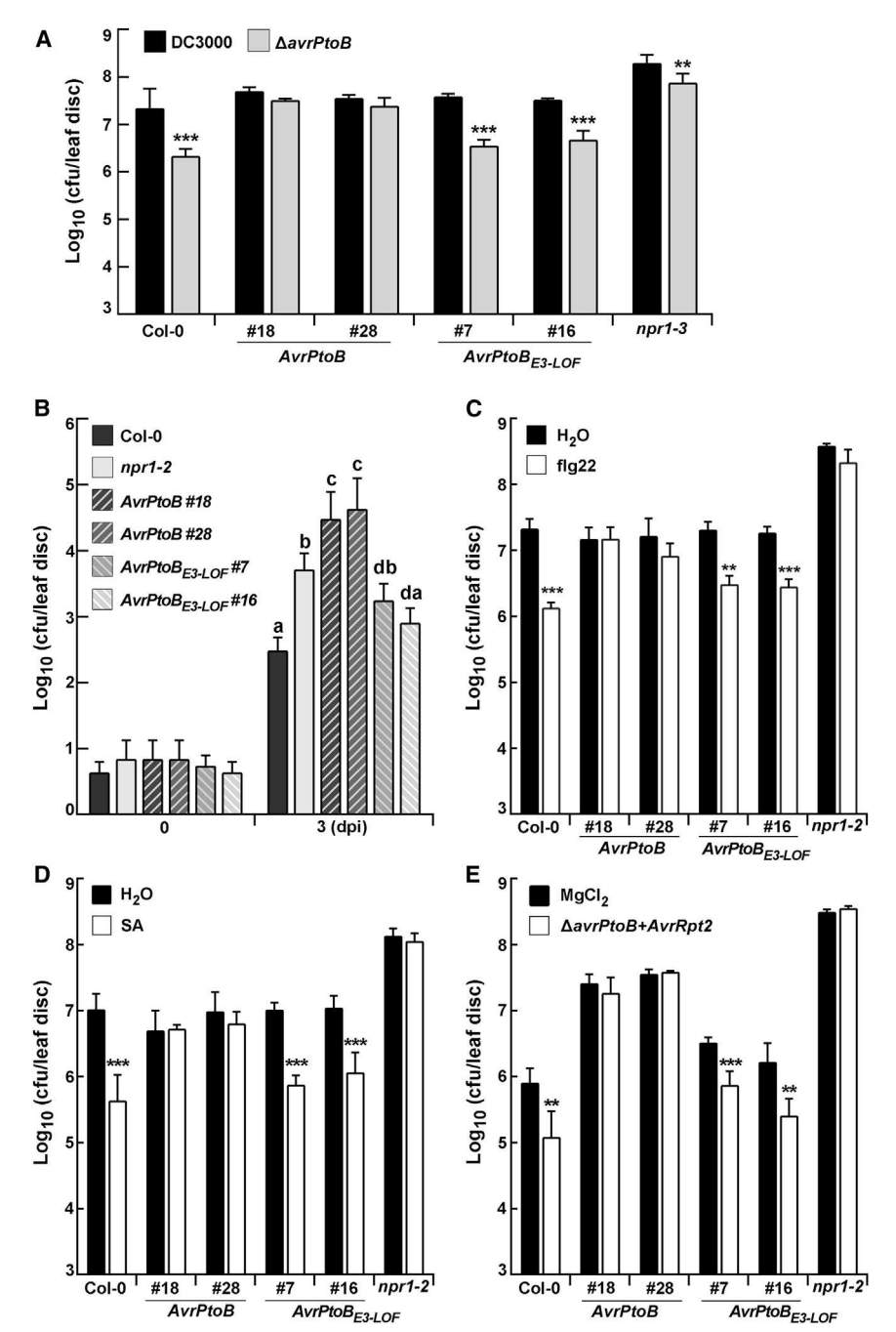
Likewise, SAR induced by the avirulent pathogen DC3000 $\Delta avrPtoB$ or Psm ES4326 carrying AvrRpt2 (Figures 5E and S5D) was abolished in systemic leaves of Arabidopsis AvrPtoB but not $AvrPtoB_{E3-LOF}$ transgenic plants, indicating that the E3 ligase activity of AvrPtoB is important for the inhibition of SAR. Furthermore, AvrPtoB but not $AvrPtoB_{E3-LOF}$ transgenic seedlings were hypersensitive to SA-induced toxicity on Murashige and Skoog plates, a phenotype resembling npr1-2 mutants (Figure S5E). Taken together, we conclude that the targeting of NPR1 by AvrPtoB in host cells could subvert NPR1-dependent SA-mediated plant defense.

NPR1 Plays a Prominent Role in MAMP Signaling

Because AvrPtoB mediates NPR1 degradation and suppresses MTI, we analyzed whether NPR1 would be regulated during

DISCUSSION

Despite the importance of NPR1 in SA signaling, it has never been shown to be a target of a pathogen effector. Our studies here show that the *bona fide* type III effector AvrPtoB, which is injected into plant cells by a *P. syringae* type III secretion system (Fu et al., 2006), directly targets the master regulator of SA



signaling NPR1 to subvert plant immunity. We find that SA promotes the interaction between NPR1 and AvrPtoB. Thus, our study reveals a paradigm in the molecular interactions between hosts and microbes. Before pathogen infection or SA treatment, most NPR1 protein exists as oligomers in the cytosol in a resting state (Kinkema et al., 2000; Mou et al., 2003). Upon pathogen infection or SA treatment, NPR1 oligomers are reduced to monomers and enter the nucleus to interact with TGA transcription factors and activate *PR* gene expression. Since AvrPtoB is also localized in the cytosol (Gohre et al., 2008), it is likely that AvrPtoB facilitates NPR1 degradation in

Figure 5. Transgenic Expression of AvrPtoB Inhibits MTI and SA-Regulated Plant Immunity Dependent on its E3 Ligase Activity

(A) Transgenic expression of AvrPtoB in Arabidopsis restores the virulence of the \(\Delta avrPtoB. \) The leaves of 5-week-old soil-grown Col-0 Arabidopsis, two independent AvrPtoB transgenic lines (Dex:Flag-AvrPtoB #18 and #28) and two independent AvrPtoB_{E3-LOF} transgenic lines (Dex:Flag-AvrPtoB_{E3-LOF} #7 and #16) were hand infiltrated with Pst DC3000 or $\Delta avrPtoB$ at 1 × 10⁶ cfu/mL and 10 nM DEX. Error bars represent SD (n = 7). (B) AvrPtoB suppresses MTI induced by DC3000 \textit{hrcC}^- mutant. Plants were sprayed with 3 μM DEX for 6 hr before infiltration with 10⁶ cfu/mL hrcC⁻. Quantifications of bacterial growth in planta were performed at 0 and 3 days post inoculation (dpi). Error bars represent SD. Different letters indicate the statistical significance (one-way ANOVA, Sidak's test; $\alpha = 0.05$, n = 6).

(C) AvrPtoB blocks flg22-induced innate immunity. Plant leaves were co-infiltrated with 10 nM DEX and 1 μ M flg22 peptide or H₂O for 24 hr prior to inoculation with DC3000 at 10⁶ cfu/mL. Bacterial multiplications were assessed at 3 dpi. Error bars represent SD (n = 4).

(D) AvrPtoB suppresses SA-mediated immunity. Plant leaves were co-sprayed with 3 μ M DEX and 0.3 mM SA or H₂O for 48 hr before infiltration using 10⁶ cfu/mL of *Psm* ES4326. Multiplication was assessed at 2 dpi. Error bars represent SD (n = 6). (E) AvrPtoB impairs SAR. Plant leaves were sprayed with 3 μ M DEX for 12 hr before inoculation with either DC3000 $\Delta avrPtoB$ AvrRpt2 (10⁷ cfu/mL) or MgCl₂ in two lower leaves. After 24 hpi, upper leaves were infiltrated with DC3000 $\Delta avrPtoB$ (10⁶ cfu/mL) and leaf discs from the second inoculation were collected 2 dpi. Error bars represent SD (n = 6).

Results are representative of at least three independent experiments. Asterisks indicate significant differences between mock and corresponding treatments (multiple t tests, one per row, $^{**}p < 0.01$, $^{***}p < 0.001$). See also Figure S5.

the cytosol prior to nuclear entry, thereby disrupting SA-mediated plant defense.

NPR1 protein in plants, which is required for the expressing of *PR* genes encoding antimicrobial proteins, is functionally equivalent to mammalian nuclear factor (NF)-κB protein, which promotes

the expression of antimicrobial cytokines (Tak and Firestein, 2001). Similar to our report, some intracellular human pathogens (Salmonella, Legionella, Shigella, etc.) also possess ubiquitin ligase-like effectors that interfere with host responses to promote infection (Ashida and Sasakawa, 2016). For example, one conserved bacterial effector NEL E3 ligase secreted by Shigella interacts with a classic NF-κB protein p65 causing poly-ubiquitination of p65 and undermining NF-κB activation in response to tumor necrosis factor alpha. Taken together, these studies indicate that plant and mammalian bacterial pathogens have evolved similar strategies to suppress the

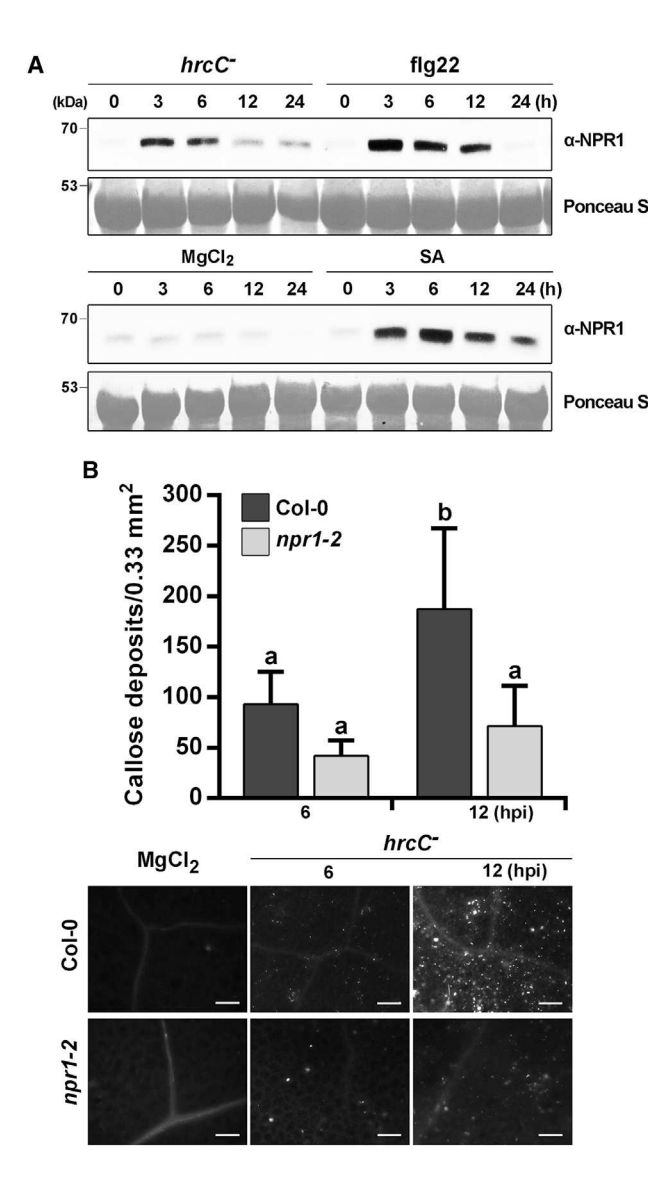


Figure 6. NPR1 Acts as a Positive Regulator of DC3000 hrcC Mutant Flicited MTI

(A) NPR1 protein is activated by multiple MAMPs. Col-0 leaves were collected at indicated time points after infiltration with 10 8 cfu/mL DC3000 $hrcC^-$ mutant, 2 μ M flg22, 10 mM MgCl $_2$, or 0.2 mM SA. Total NPR1 protein was analyzed by immunoblot using $\alpha\textsc{-NPR1}$ antibody.

(B) NPR1 regulates callose deposition in response to DC3000 $hrcC^-$. Plant leaves were infiltrated with 10^8 cfu/mL $hrcC^-$ mutant and callose deposition was quantified at 6 and 12 hpi (top). Error bars represent SD. Different letters indicate the statistical significance (two-way ANOVA, Tukey's multiple test; α = 0.05, n = 9). Representative images are shown (bottom). Scale bar, 100 μ m. See also Figure S6.

central defense mechanism of their corresponding hosts to establish infection.

In this study, NPR1 is identified as a target of the type III effector AvrPtoB. AvrPtoB was previously shown to interact with Pto kinase, another Pto family protein Fen kinase and a LysM receptor-like kinase Bti9 in tomato (Kim et al., 2002; Rosebrock et al., 2007; Zeng et al., 2012). Also, the potent effector AvrPtoB targets flagellin co-receptors FLS2/BAK1 and chitin re-

ceptor CERK1 to suppress MTI in Arabidopsis (Gohre et al., 2008; Shan et al., 2008; Gimenez-Ibanez et al., 2009). Therefore, AvrPtoB has here been shown to target both MAMP receptors and the master regulator of plant defense NPR1. These findings indicate that AvrPtoB has multiple targets in host cells and targets distinct components involved in plant defense (Cheng et al., 2011; Wei et al., 2015). Thus, we speculate that more unknown regulators important for plant immunity might be targets of AvrPtoB in Arabidopsis. NPR1, as a target of AvrPtoB, is a central hub for transcriptional reprogramming in SA-modulated host immunity. Given that plants have evolved a large array of PRRs for recognizing specific ligands that elicit plant defense responses, it is likely that pathogen effectors blocking downstream convergent signaling components in MTI could provide an effective strategy to suppress different routes of MTIs. These intricate molecular and functional features not only reflect a co-evolutionary tug of war in host-pathogen interactions but also suggest that effectors have evolved to interfere with the most critical hubs in the plant defense network.

To further elucidate the mechanisms of NPR1 in mediating MTI responses, in-depth studies will focus on identifying the specific MAMP and/or multiple MAMPs signaling implicated in NPR1regulated innate immunity. Our data mainly illustrate that AvrPtoB efficiently degrades NPR1 and in turn disturbs the expression of NPR1-dependent SA signaling genes involved in callose biosynthesis and PR1. Notably, several NPR1-dependent MAMP response genes induced by hrcC- (Figure S6C) are also found to be upregulated in SA signaling (Wang et al., 2006), which have been shown to be attenuated by the conditional expression of AvrPtoB in a previous study (de Torres et al., 2006). Thus, AvrPtoB could suppress NPR1-dependent transcriptional reprogramming during SA-mediated immune responses. To detect the global NPR1-dependent transcription reprogramming affected by AvrPtoB, it will be of interest to determine the degree of overlap among genes misregulated in AvrPtoB transgenic lines and npr1 plants upon DC3000 hrcCmutant treatment.

STAR*METHODS

Detailed methods are provided in the online version of this paper and include the following:

- KEY RESOURCES TABLE
- CONTACT FOR REAGENT AND RESOURCE SHARING
- EXPERIMENTAL MODEL AND SUBJECT DETAILS
 - Arabidopsis
 - Nicotiana benthamiana
 - Bacterial Strains
- METHOD DETAILS
 - Plasmid Construction
 - Yeast Two-Hybrid Screens
 - Yeast Protein Extraction
 - Recombinant Protein Purification
 - O GST Pull-Down Assay
 - Plant Protein Extraction and Immunoblotting
 - Co-Immunoprecipitation (Co-IP) Assay
 - Ubiquitination Assay
 - Agrobacterium-Mediated Transient Assay

- Callose Staining and Quantification
- O NPR1-GFP Distribution and Quantification
- Pathogenicity Tests
- O Induction of AvrPtoB in Minimal Medium
- Gene Expression Analysis
- QUANTIFICATION AND STATISTICAL ANALYSIS

SUPPLEMENTAL INFORMATION

Supplemental Information includes six figures and one table and can be found with this article online at https://doi.org/10.1016/j.chom.2017.10.019.

AUTHOR CONTRIBUTIONS

H.C., F.L., and Z.Q.F. designed experiments and analyzed data. H.C. performed most of the experiments and prepared the figures. J.C., M.L., M.C., K.X., Z.S., Y. Zhao, I.P., Y. Zheng, and J.M. performed the remainder of the experiments. J.R.A. and M.T.N. provided many of the bacterial strains and constructs used in this study. H.C., Z.Q.F., and F.L. wrote the paper with inputs from other authors.

ACKNOWLEDGMENTS

We thank Jeff Dangl for providing *P. syringae* type III effector entry clones; Greg Martin and Ping He for providing *P. syringae* pv. tomato DC3000 Δ*avrPtoB* mutant and DC3000 Δ*avrPtoB* Δ*avrPto* double mutant; Libo Shan for providing Nd-0 *AvrPtoB* transgenic plants; Zhonglin Mou for providing *pad4* and *eds5* mutant seeds; and Xinnian Dong, Beth Krizek, and Johannes Stratmann for critical reading of this manuscript. M.L. was partly funded by the Chinese Scholarship Council.

Received: April 22, 2017 Revised: July 10, 2017 Accepted: October 25, 2017 Published: November 22, 2017

REFERENCES

Ashida, H., and Sasakawa, C. (2016). Bacterial E3 ligase effectors exploit host ubiquitin systems. Curr. Opin. Microbiol. 35, 16–22.

Baltrus, D.A., Nishimura, M.T., Romanchuk, A., Chang, J.H., Mukhtar, M.S., Cherkis, K., Roach, J., Grant, S.R., Jones, C.D., and Dangl, J.L. (2011). Dynamic evolution of pathogenicity revealed by sequencing and comparative genomics of 19 *Pseudomonas syringae* isolates. PLoS Pathog. 7, e1002132.

Bartsch, M., Gobbato, E., Bednarek, P., Debey, S., Schultze, J.L., Bautor, J., and Parker, J.E. (2006). Salicylic acid-independent ENHANCED DISEASE SUSCEPTIBILITY1 signaling in Arabidopsis immunity and cell death is regulated by the monooxygenase FMO1 and the Nudix hydrolase NUDT7. Plant Cell 18, 1038–1051.

Block, A., Li, G., Fu, Z.Q., and Alfano, J.R. (2008). Phytopathogen type III effector weaponry and their plant targets. Curr. Opin. Plant Biol. 11, 396–403.

Boller, T., and Felix, G. (2009). A renaissance of elicitors: perception of microbe-associated molecular patterns and danger signals by pattern-recognition receptors. Annu. Rev. Plant Biol. *60*, 379–406.

Caillaud, M.C., Asai, S., Rallapalli, G., Piquerez, S., Fabro, G., and Jones, J.D. (2013). A downy mildew effector attenuates salicylic acid-triggered immunity in *Arabidopsis* by interacting with the host mediator complex. PLoS Biol. *11*, e1001732

Cao, H., Bowling, S.A., Gordon, A.S., and Dong, X. (1994). Characterization of an *Arabidopsis* mutant that is nonresponsive to inducers of systemic acquired resistance. Plant Cell *6*, 1583–1592.

Cao, H., Glazebrook, J., Clarke, J.D., Volko, S., and Dong, X. (1997). The Arabidopsis NPR1 gene that controls systemic acquired resistance encodes a novel protein containing ankyrin repeats. Cell *88*, 57–63.

Chang, J.H., Urbach, J.M., Law, T.F., Arnold, L.W., Hu, A., Gombar, S., Grant, S.R., Ausubel, F.M., and Dangl, J.L. (2005). A high-throughput, near-saturating screen for type III effector genes from *Pseudomonas syringae*. Proc. Natl. Acad. Sci. USA *102*, 2549–2554.

Chen, Z., Zheng, Z., Huang, J., Lai, Z., and Fan, B. (2009). Biosynthesis of salicylic acid in plants. Plant Signal. Behav. 4, 493–496.

Cheng, W., Munkvold, K.R., Gao, H., Mathieu, J., Schwizer, S., Wang, S., Yan, Y.B., Wang, J., Martin, G.B., and Chai, J. (2011). Structural analysis of *Pseudomonas syringae* AvrPtoB bound to host BAK1 reveals two similar kinase-interacting domains in a type III Effector. Cell Host Microbe *10*, 616–626.

de Torres, M., Mansfield, J.W., Grabov, N., Brown, I.R., Ammouneh, H., Tsiamis, G., Forsyth, A., Robatzek, S., Grant, M., and Boch, J. (2006). *Pseudomonas syringae* effector AvrPtoB suppresses basal defence in Arabidopsis. Plant J. 47, 368–382.

DebRoy, S., Thilmony, R., Kwack, Y.B., Nomura, K., and He, S.Y. (2004). A family of conserved bacterial effectors inhibits salicylic acid-mediated basal immunity and promotes disease necrosis in plants. Proc. Natl. Acad. Sci. USA 101, 9927–9932.

Delaney, T.P., Uknes, S., Vernooij, B., Friedrich, L., Weymann, K., Negrotto, D., Gaffney, T., Gut-Rella, M., Kessmann, H., Ward, E., et al. (1994). A central role of salicylic acid in plant disease resistance. Science 266, 1247–1250.

Djamei, A., Schipper, K., Rabe, F., Ghosh, A., Vincon, V., Kahnt, J., Osorio, S., Tohge, T., Fernie, A.R., Feussner, I., et al. (2011). Metabolic priming by a secreted fungal effector. Nature *478*, 395–398.

Dong, X., Hong, Z., Chatterjee, J., Kim, S., and Verma, D.P. (2008). Expression of callose synthase genes and its connection with Npr1 signaling pathway during pathogen infection. Planta 229, 87–98.

Fu, Z.Q., and Dong, X. (2013). Systemic acquired resistance: turning local infection into global defense. Annu. Rev. Plant Biol. 64, 839–863.

Fu, Z.Q., Guo, M., and Alfano, J.R. (2006). *Pseudomonas syringae* HrpJ is a type III secreted protein that is required for plant pathogenesis, injection of effectors, and secretion of the HrpZ1 Harpin. J. Bacteriol. *188*, 6060–6069.

Fu, Z.Q., Guo, M., Jeong, B.R., Tian, F., Elthon, T.E., Cerny, R.L., Staiger, D., and Alfano, J.R. (2007). A type III effector ADP-ribosylates RNA-binding proteins and quells plant immunity. Nature 447, 284–288.

Fu, Z.Q., Yan, S., Saleh, A., Wang, W., Ruble, J., Oka, N., Mohan, R., Spoel, S.H., Tada, Y., Zheng, N., et al. (2012). NPR3 and NPR4 are receptors for the immune signal salicylic acid in plants. Nature 486, 228–232.

Galan, J.E., and Collmer, A. (1999). Type III secretion machines: bacterial devices for protein delivery into host cells. Science 284, 1322–1328.

Gimenez-Ibanez, S., Hann, D.R., Ntoukakis, V., Petutschnig, E., Lipka, V., and Rathjen, J.P. (2009). AvrPtoB targets the LysM receptor kinase CERK1 to promote bacterial virulence on plants. Curr. Biol. 19, 423–429.

Gohre, V., Spallek, T., Haweker, H., Mersmann, S., Mentzel, T., Boller, T., De Torres, M., Mansfield, J.W., and Robatzek, S. (2008). Plant pattern-recognition receptor FLS2 is directed for degradation by the bacterial ubiquitin ligase AvrPtoB. Curr. Biol. *18*, 1824–1832.

Gomez-Gomez, L., Felix, G., and Boller, T. (1999). A single locus determines sensitivity to bacterial flagellin in *Arabidopsis thaliana*. Plant J. 18, 277–284.

Guo, M., Tian, F., Wamboldt, Y., and Alfano, J.R. (2009). The majority of the type III effector inventory of *Pseudomonas syringae pv. tomato* DC3000 can suppress plant immunity. Mol. Plant Microbe Interact. *22*, 1069–1080.

Hauck, P., Thilmony, R., and He, S.Y. (2003). A *Pseudomonas syringae* type III effector suppresses cell wall-based extracellular defense in susceptible *Arabidopsis* plants. Proc. Natl. Acad. Sci. USA *100*, 8577–8582.

Jelenska, J., Yao, N., Vinatzer, B.A., Wright, C.M., Brodsky, J.L., and Greenberg, J.T. (2007). A J domain virulence effector of *Pseudomonas syringae* remodels host chloroplasts and suppresses defenses. Curr. Biol. 17, 499–508

Jirage, D., Tootle, T.L., Reuber, T.L., Frost, L.N., Feys, B.J., Parker, J.E., Ausubel, F.M., and Glazebrook, J. (1999). *Arabidopsis thaliana* PAD4 encodes a lipase-like gene that is important for salicylic acid signaling. Proc. Natl. Acad. Sci. USA *96*, 13583–13588.

Jones, J.D., and Dangl, J.L. (2006). The plant immune system. Nature 444, 323-329

Kim, Y.J., Lin, N.C., and Martin, G.B. (2002). Two distinct Pseudomonas effector proteins interact with the Pto kinase and activate plant immunity. Cell 109, 589-598.

Kinkema, M., Fan, W., and Dong, X. (2000). Nuclear localization of NPR1 is required for activation of PR gene expression. Plant Cell 12, 2339-2350.

Lin, N.C., and Martin, G.B. (2005). An avrPto/avrPtoB mutant of Pseudomonas syringae pv. tomato DC3000 does not elicit Pto-mediated resistance and is less virulent on tomato. Mol. Plant Microbe Interact. 18, 43-51.

Lindeberg, M., Cunnac, S., and Collmer, A. (2012). Pseudomonas syringae type III effector repertoires: last words in endless arguments. Trends Microbiol. 20, 199-208.

Liu, T., Song, T., Zhang, X., Yuan, H., Su, L., Li, W., Xu, J., Liu, S., Chen, L., Chen, T., et al. (2014). Unconventionally secreted effectors of two filamentous pathogens target plant salicylate biosynthesis. Nat. Commun. 5, 4686.

Lu, H. (2009). Dissection of salicylic acid-mediated defense signaling networks. Plant Signal. Behav. 4, 713-717.

Mathieu, J., Schwizer, S., and Martin, G.B. (2014). Pto kinase binds two domains of AvrPtoB and its proximity to the effector E3 ligase determines if it evades degradation and activates plant immunity. PLoS Pathog. 10, e1004227.

Mou, Z., Fan, W., and Dong, X. (2003). Inducers of plant systemic acquired resistance regulate NPR1 function through redox changes. Cell 113, 935-944.

Mukhtar, M.S., Carvunis, A.R., Dreze, M., Epple, P., Steinbrenner, J., Moore, J., Tasan, M., Galli, M., Hao, T., Nishimura, M.T., et al. (2011). Independently evolved virulence effectors converge onto hubs in a plant immune system network, Science 333, 596-601.

Nawrath, C., Heck, S., Parinthawong, N., and Metraux, J.P. (2002). EDS5, an essential component of salicylic acid-dependent signaling for disease resistance in Arabidopsis, is a member of the MATE transporter family. Plant Cell 14, 275-286.

Rosebrock, T.R., Zeng, L., Brady, J.J., Abramovitch, R.B., Xiao, F., and Martin, G.B. (2007). A bacterial E3 ubiquitin ligase targets a host protein kinase to disrupt plant immunity. Nature 448, 370-374.

Salmeron, J.M., Oldroyd, G.E., Rommens, C.M., Scofield, S.R., Kim, H.S., Lavelle, D.T., Dahlbeck, D., and Staskawicz, B.J. (1996). Tomato Prf is a member of the leucine-rich repeat class of plant disease resistance genes and lies embedded within the Pto kinase gene cluster. Cell 86, 123-133.

Shah, J., Tsui, F., and Klessig, D.F. (1997). Characterization of a salicylic acidinsensitive mutant (sai1) of Arabidopsis thaliana, identified in a selective screen utilizing the SA-inducible expression of the tms2 gene. Mol. Plant Microbe Interact. 10, 69-78.

Shan, L., He, P., Li, J., Heese, A., Peck, S.C., Nurnberger, T., Martin, G.B., and Sheen, J. (2008). Bacterial effectors target the common signaling partner BAK1 to disrupt multiple MAMP receptor-signaling complexes and impede plant immunity. Cell Host Microbe 4, 17-27.

Spoel, S.H., Mou, Z., Tada, Y., Spivey, N.W., Genschik, P., and Dong, X. (2009). Proteasome-mediated turnover of the transcription coactivator NPR1 plays dual roles in regulating plant immunity. Cell 137, 860-872.

Sun, Y., Li, L., Macho, A.P., Han, Z., Hu, Z., Zipfel, C., Zhou, J.M., and Chai, J. (2013). Structural basis for flg22-induced activation of the Arabidopsis FLS2-BAK1 immune complex. Science 342, 624-628.

Tada, Y., Spoel, S.H., Pajerowska-Mukhtar, K., Mou, Z., Song, J., Wang, C., Zuo, J., and Dong, X. (2008). Plant immunity requires conformational changes of NPR1 via S-nitrosylation and thioredoxins. Science 321, 952-956.

Tak, P.P., and Firestein, G.S. (2001). NF-kappaB: a key role in inflammatory diseases. J. Clin. Invest. 107, 7-11.

Tanaka, S., Han, X., and Kahmann, R. (2015). Microbial effectors target multiple steps in the salicylic acid production and signaling pathway. Front. Plant Sci 6 349

Tsuda, K., and Katagiri, F. (2010). Comparing signaling mechanisms engaged in pattern-triggered and effector-triggered immunity. Curr. Opin. Plant Biol. 13,

Wang, D., Amornsiripanitch, N., and Dong, X. (2006). A genomic approach to identify regulatory nodes in the transcriptional network of systemic acquired resistance in plants. PLoS Pathog. 2, e123.

Wei, H.L., Chakravarthy, S., Mathieu, J., Helmann, T.C., Stodghill, P., Swingle, B., Martin, G.B., and Collmer, A. (2015). Pseudomonas syringae pv. tomato DC3000 type III secretion effector polymutants reveal an interplay between HopAD1 and AvrPtoB. Cell Host Microbe 17, 752-762.

Wildermuth, M.C., Dewdney, J., Wu, G., and Ausubel, F.M. (2001). Isochorismate synthase is required to synthesize salicylic acid for plant defence. Nature 414, 562-565.

Wirthmueller, L., Maqbool, A., and Banfield, M.J. (2013). On the front line: structural insights into plant-pathogen interactions. Nat. Rev. Microbiol. 11, 761-776.

Wu, L., Chen, H., Curtis, C., and Fu, Z.Q. (2014). Go in for the kill: how plants deploy effector-triggered immunity to combat pathogens. Virulence 5,

Xiao, F., He, P., Abramovitch, R.B., Dawson, J.E., Nicholson, L.K., Sheen, J., and Martin, G.B. (2007). The N-terminal region of Pseudomonas type III effector AvrPtoB elicits Pto-dependent immunity and has two distinct virulence determinants. Plant J. 52, 595-614.

Zeng, L., Velasquez, A.C., Munkvold, K.R., Zhang, J., and Martin, G.B. (2012). A tomato LysM receptor-like kinase promotes immunity and its kinase activity is inhibited by AvrPtoB. Plant J. 69, 92-103.

STAR***METHODS**

KEY RESOURCES TABLE

REAGENT or RESOURCE	SOURCE	IDENTIFIER
Antibodies		
Mouse monoclonal anti-GFP (JL-8)	Clontech	Cat# 632381; RRID:AB_2313808)
Mouse monoclonal anti-FLAG M2-Peroxidase (HRP)	Sigma-Aldrich	Cat# A8592; RRID:AB_439702
Rat monoclonal anti-HA-Peroxidase (3F10)	Roche	Cat# 12013819001; RRID:AB_390917
Goat polyclonal anti-GST antibody	GE Healthcare	Cat# 27-4577-01; RRID:AB_771432
Mouse monoclonal anti-His antibody	GenScript	Cat# A00186; RRID:AB_914704
Mouse monoclonal anti-c-Myc antibody	ThermoFisher	Cat# R950-25; RRID:AB_2556560
Rabbit polyclonal anti-NPR1 antibody	Agrisera	Cat# AS12 1854
Rabbit polyclonal anti-PR1 antibody	Agrisera	Cat# AS10 687; RRID:AB_1075175
Rabbit polyclonal anti-UBQ11 ubiquitin antibody	Agrisera	Cat# AS08 307A; RRID:AB_2256904
Alpaca anti-GFP coupled to magnetic agarose beads	Chromotek	Cat# GFP-Trap®_MA gtma-20; RRID: AB_2631357
Mouse monoclonal anti-FLAG M2 magnetic beads	Sigma-Aldrich	Cat# M8823; RRID: AB_2637089
Bacterial and Virus Strains		
Pst DC3000 ΔavrPtoB	Lin and Martin, 2005	N/A
Pst DC3000 ΔavrPto	Lin and Martin, 2005	N/A
Pst DC3000 ΔavrPtoB, ΔavrPto	Lin and Martin, 2005	N/A
P. fluorescens AvrPtoB	This paper	N/A
P. fluorescens AvrPtoB _{E3-LOF}	This paper	N/A
E. coli C41 (DE3) pLysS	Lucigen	Cat# 60444-1
Chemicals, Peptides, and Recombinant Proteins		
Gateway BP Clonase II Enzyme Mix	ThermoFisher	Cat# 11789-100;
Gateway LR Clonase II Enzyme Mix	ThermoFisher	Cat# 11791-100
Dexamethasone	Sigma-Aldrich	Cat# D1756-25MG; CAS: 50-02-2
Protease inhibitor cocktail	Sigma-Aldrich	Cat# P9599-5ML
MG115 proteasome inhibitor	Sigma-Aldrich	Cat# C6706-5MG; CAS:133407-86-0
Sodium salicylate (SA)	Sigma-Aldrich	Cat# S3007-1KG; CAS: 54-21-7
3,5-Dichlorosalicylic acid (DCSA)	Alfa Aesar	Cat# B23641; CAS: 320-72-9
2,6-Dichloropyridine-4-carboxylic acid (INA)	Matrix Scientific	Cat# 011178; CAS: 5398-44-7
3-Hydroxybenzoin acid (3HBA)	Alfa Aesar	Cat# A13628; CAS: 99-06-9
Methyl blue (Aniline blue)	Alfa Aesar	Cat# H37721; CAS: 28983-56-4
Bafilomycin A1	BioViotica	Cat# BVT-0252-C100
cOmplete mini EDTA-free protease inhibitor cocktail	Roche	Cat# 11836170001
PhosSTOP inhibitor	Roche	Cat# 04-906-837-001
Benzonase Nuclease	EMD Millipore	Cat# 70746-3
Phusion High-Fidelity DNA Polymerase	NEB	Cat# M0530L
PfuTurbo DNA Polymerase	Agilent	Cat# 600252
Flgelin22 (Flg22)	GenScript	Cat# RP19986
Critical Commercial Assays		
pENTR Directional TOPO Cloning Kit	Thermo Fisher	Cat# K2400-20
BugBuster Protein Extraction Reagent	EMD Millipore	Cat# 70584-4

(Continued on next page)



Continued		
REAGENT or RESOURCE	SOURCE	IDENTIFIER
MagneGST Protein Purification System	Promega	Cat# V8603
MagneHis Protein Purification System	Promega	Cat# V8550
QIAprep Spin Miniprep	Qiagen	Cat# 27115
RNeasy Plant Mini Kit	Qiagen	Cat# 74904
GoTaq Green Master Mix	Promega	Cat# M7122
SuperScript III First-Strand Synthesis System	ThermoFisher	Cat# 18080-051
Power SYBR Green PCR Master Mix	ThermoFisher	Cat# 4367659
Experimental Models: Organisms/Strains		
Arabidopsis: 35S:NPR1-GFP/npr1-2	Mou et al., 2003	N/A
Arabidopsis: Dex:Flag-AvrPtoB	This study	N/A
Arabidopsis: Dex:Flag-AvrPtoB;35S:NPR1-GFP/npr1-2	This study	N/A
Arabidopsis: Dex:Flag-AvrPtoB _{E3-LOF}	This study	N/A
Arabidopsis: Dex:AvrPtoB	de Torres et al., 2006	N/A
Arabidopsis: npr1-2,	Cao et al., 1997	N/A
Arabidopsis: npr1-3	Arabidopsis Biological Resource Center	N/A
Arabidopsis: ics1	Wildermuth et al., 2001	N/A
Arabidopsis: eds5	Nawrath et al., 2002	N/A
Arabidopsis: eds1-2	Bartsch et al., 2006	N/A
Arabidopsis: pad4	Jirage et al., 1999	N/A
Arabidopsis: fls2	Arabidopsis Biological Resource Center	N/A
N. benthamiana: NahG	Delaney et al., 1994	N/A
Oligonucleotides	,	
Primers used in this study, see Table S1	This paper	N/A
Recombinant DNA		
Recombinant DNA pDEST-GBKT7-AvrPtoB	This paper	N/A
	This paper This paper	N/A N/A
pDEST-GBKT7-AvrPtoB		
pDEST-GBKT7-AvrPtoB pDEST-GADT7-NPR1 pDEST-GADT7-GUS	This paper	N/A
pDEST-GBKT7-AvrPtoB pDEST-GADT7-NPR1 pDEST-GADT7-GUS	This paper This paper	N/A N/A
pDEST-GBKT7-AvrPtoB pDEST-GADT7-NPR1 pDEST-GADT7-GUS pDEST-GBKT7-AvrPtoB ₁₋₂₀₅ pDEST-GBKT7-AvrPtoB ₁₋₃₀₇	This paper This paper This paper	N/A N/A N/A
pDEST-GBKT7-AvrPtoB pDEST-GADT7-NPR1 pDEST-GADT7-GUS pDEST-GBKT7-AvrPtoB ₁₋₂₀₅ pDEST-GBKT7-AvrPtoB ₁₋₃₀₇ pDEST-GBKT7-AvrPtoB ₁₋₃₈₇	This paper This paper This paper This paper	N/A N/A N/A N/A
pDEST-GBKT7-AvrPtoB pDEST-GADT7-NPR1 pDEST-GADT7-GUS pDEST-GBKT7-AvrPtoB ₁₋₂₀₅ pDEST-GBKT7-AvrPtoB ₁₋₃₀₇ pDEST-GBKT7-AvrPtoB ₁₋₃₈₇	This paper This paper This paper This paper This paper This paper	N/A N/A N/A N/A
pDEST-GBKT7-AvrPtoB pDEST-GADT7-NPR1 pDEST-GADT7-GUS pDEST-GBKT7-AvrPtoB ₁₋₂₀₅ pDEST-GBKT7-AvrPtoB ₁₋₃₀₇ pDEST-GBKT7-AvrPtoB ₁₋₃₈₇ pDEST-GBKT7-AvrPtoB _{E3-LOF} pDEST-GBKT7-AvrPtoB ₃₀₈₋₄₃₆	This paper	N/A N/A N/A N/A N/A N/A N/A
pDEST-GBKT7-AvrPtoB pDEST-GADT7-NPR1 pDEST-GADT7-GUS pDEST-GBKT7-AvrPtoB ₁₋₂₀₅ pDEST-GBKT7-AvrPtoB ₁₋₃₀₇ pDEST-GBKT7-AvrPtoB ₁₋₃₈₇ pDEST-GBKT7-AvrPtoB _{2-LOF} pDEST-GBKT7-AvrPtoB ₃₀₈₋₄₃₆ pDEST-GBKT7-AvrPtoB ₃₀₈₋₅₅₃	This paper	N/A
pDEST-GBKT7-AvrPtoB pDEST-GADT7-NPR1 pDEST-GADT7-GUS pDEST-GBKT7-AvrPtoB ₁₋₂₀₅ pDEST-GBKT7-AvrPtoB ₁₋₃₀₇ pDEST-GBKT7-AvrPtoB ₁₋₃₈₇ pDEST-GBKT7-AvrPtoB _{5-LOF} pDEST-GBKT7-AvrPtoB ₃₀₈₋₄₃₆ pDEST-GBKT7-AvrPtoB ₃₀₈₋₅₅₃ pDEST-GBKT7-AvrPto	This paper	N/A N/A N/A N/A N/A N/A N/A N/A
pDEST-GBKT7-AvrPtoB pDEST-GADT7-NPR1 pDEST-GADT7-GUS pDEST-GBKT7-AvrPtoB ₁₋₂₀₅ pDEST-GBKT7-AvrPtoB ₁₋₃₀₇ pDEST-GBKT7-AvrPtoB ₁₋₃₈₇ pDEST-GBKT7-AvrPtoB _{23-LOF} pDEST-GBKT7-AvrPtoB ₃₀₈₋₄₃₆ pDEST-GBKT7-AvrPtoB ₃₀₈₋₅₅₃ pDEST-GBKT7-AvrPto pDEST-GBKT7-AvrPto	This paper	N/A
pDEST-GBKT7-AvrPtoB pDEST-GADT7-NPR1 pDEST-GADT7-GUS pDEST-GBKT7-AvrPtoB ₁₋₂₀₅ pDEST-GBKT7-AvrPtoB ₁₋₃₀₇ pDEST-GBKT7-AvrPtoB ₁₋₃₈₇ pDEST-GBKT7-AvrPtoB _{5-LOF} pDEST-GBKT7-AvrPtoB ₃₀₈₋₄₃₆ pDEST-GBKT7-AvrPtoB ₃₀₈₋₅₅₃ pDEST-GBKT7-AvrPto pDEST-GADT7-NPR1 ₁₋₂₈₀ pDEST-GADT7-NPR1 ₁₅₀₋₅₉₃	This paper	N/A
pDEST-GBKT7-AvrPtoB pDEST-GADT7-NPR1 pDEST-GADT7-GUS pDEST-GBKT7-AvrPtoB ₁₋₂₀₅ pDEST-GBKT7-AvrPtoB ₁₋₃₀₇ pDEST-GBKT7-AvrPtoB ₁₋₃₈₇ pDEST-GBKT7-AvrPtoB _{5-1.05} pDEST-GBKT7-AvrPtoB ₃₀₈₋₄₃₆ pDEST-GBKT7-AvrPtoB ₃₀₈₋₅₅₃ pDEST-GBKT7-AvrPto pDEST-GBKT7-AvrPto pDEST-GADT7-NPR1 ₁₋₂₈₀ pDEST-GADT7-NPR1 ₁₅₀₋₅₉₃ pDEST-GADT7-nim1-2	This paper	N/A
pDEST-GBKT7-AvrPtoB pDEST-GADT7-NPR1 pDEST-GADT7-GUS pDEST-GBKT7-AvrPtoB ₁₋₂₀₅ pDEST-GBKT7-AvrPtoB ₁₋₃₀₇ pDEST-GBKT7-AvrPtoB ₁₋₃₈₇ pDEST-GBKT7-AvrPtoB _{53-LOF} pDEST-GBKT7-AvrPtoB ₃₀₈₋₄₃₆ pDEST-GBKT7-AvrPtoB ₃₀₈₋₅₅₃ pDEST-GBKT7-AvrPto pDEST-GBKT7-AvrPto pDEST-GADT7-NPR1 ₁₋₂₈₀ pDEST-GADT7-nim1-2 pDEST-GADT7-npr1-1	This paper	N/A
pDEST-GBKT7-AvrPtoB pDEST-GADT7-NPR1 pDEST-GADT7-GUS pDEST-GBKT7-AvrPtoB ₁₋₂₀₅ pDEST-GBKT7-AvrPtoB ₁₋₃₀₇ pDEST-GBKT7-AvrPtoB ₁₋₃₈₇ pDEST-GBKT7-AvrPtoB _{5-1.05} pDEST-GBKT7-AvrPtoB ₃₀₈₋₄₃₆ pDEST-GBKT7-AvrPtoB ₃₀₈₋₅₅₃ pDEST-GBKT7-AvrPto pDEST-GADT7-NPR1 ₁₋₂₈₀ pDEST-GADT7-NPR1 ₁₅₀₋₅₉₃ pDEST-GADT7-nim1-2 pDEST-GADT7-npr1-1	This paper	N/A
pDEST-GBKT7-AvrPtoB pDEST-GADT7-NPR1 pDEST-GADT7-GUS pDEST-GBKT7-AvrPtoB ₁₋₂₀₅ pDEST-GBKT7-AvrPtoB ₁₋₃₀₇ pDEST-GBKT7-AvrPtoB ₁₋₃₈₇ pDEST-GBKT7-AvrPtoB _{5-1,05} pDEST-GBKT7-AvrPtoB ₃₀₈₋₄₃₆ pDEST-GBKT7-AvrPtoB ₃₀₈₋₅₅₃ pDEST-GBKT7-AvrPto pDEST-GADT7-NPR1 ₁₋₂₈₀ pDEST-GADT7-NPR1 ₁₅₀₋₅₉₃ pDEST-GADT7-nim1-2 pDEST-GADT7-npr1-1 pDEST-GADT7-npr1-5 pDEST-GADT7-NPR1ΔAKR	This paper	N/A
pDEST-GBKT7-AvrPtoB pDEST-GADT7-NPR1 pDEST-GADT7-GUS pDEST-GBKT7-AvrPtoB ₁₋₂₀₅ pDEST-GBKT7-AvrPtoB ₁₋₃₀₇ pDEST-GBKT7-AvrPtoB ₁₋₃₈₇ pDEST-GBKT7-AvrPtoB _{5-LOF} pDEST-GBKT7-AvrPtoB ₃₀₈₋₄₃₆ pDEST-GBKT7-AvrPtoB ₃₀₈₋₅₅₃ pDEST-GBKT7-AvrPto pDEST-GADT7-NPR1 ₁₋₂₈₀ pDEST-GADT7-NPR1 ₁₅₀₋₅₉₃ pDEST-GADT7-nim1-2 pDEST-GADT7-npr1-1 pDEST-GADT7-NPR1ΔAKR pDEST-GADT7-NPR1ΔAKR	This paper	N/A
pDEST-GBKT7-AvrPtoB pDEST-GADT7-NPR1 pDEST-GADT7-GUS pDEST-GBKT7-AvrPtoB ₁₋₂₀₅ pDEST-GBKT7-AvrPtoB ₁₋₃₀₇ pDEST-GBKT7-AvrPtoB ₁₋₃₈₇ pDEST-GBKT7-AvrPtoB _{2-LOF} pDEST-GBKT7-AvrPtoB ₃₀₈₋₄₃₆ pDEST-GBKT7-AvrPtoB ₃₀₈₋₅₅₃ pDEST-GBKT7-AvrPto pDEST-GADT7-NPR1 ₁₋₂₈₀ pDEST-GADT7-NPR1 ₁₅₀₋₅₉₃ pDEST-GADT7-nim1-2 pDEST-GADT7-npr1-1 pDEST-GADT7-npr1-5 pDEST-GADT7-NPR1ΔAKR pDEST-GADT7-NPR1C521A pDEST-GADT7-NPR1C529A	This paper	N/A
pDEST-GBKT7-AvrPtoB pDEST-GADT7-NPR1 pDEST-GADT7-GUS pDEST-GBKT7-AvrPtoB ₁₋₂₀₅ pDEST-GBKT7-AvrPtoB ₁₋₃₀₇ pDEST-GBKT7-AvrPtoB ₁₋₃₈₇ pDEST-GBKT7-AvrPtoB _{5-1-OF} pDEST-GBKT7-AvrPtoB ₃₀₈₋₄₃₆ pDEST-GBKT7-AvrPtoB ₃₀₈₋₅₅₃ pDEST-GBKT7-AvrPto pDEST-GBKT7-AvrPto pDEST-GADT7-NPR1 ₁₋₂₈₀ pDEST-GADT7-NPR1 ₁₅₀₋₅₉₃ pDEST-GADT7-nim1-2 pDEST-GADT7-npr1-1 pDEST-GADT7-NPR1ΔAKR pDEST-GADT7-NPR1C521A pDEST-GADT7-NPR1C529A pGEX-2TK GST	This paper	N/A
pDEST-GADT7-AvrPtoB pDEST-GADT7-FQUS pDEST-GBKT7-AvrPtoB ₁₋₂₀₅ pDEST-GBKT7-AvrPtoB ₁₋₃₀₇ pDEST-GBKT7-AvrPtoB ₁₋₃₈₇ pDEST-GBKT7-AvrPtoB ₁₋₃₈₇ pDEST-GBKT7-AvrPtoB _{2-1.0F} pDEST-GBKT7-AvrPtoB ₃₀₈₋₄₃₆ pDEST-GBKT7-AvrPtoB ₃₀₈₋₅₅₃ pDEST-GBKT7-AvrPto pDEST-GADT7-NPR1 ₁₋₂₈₀ pDEST-GADT7-NPR1 ₁₋₂₈₀ pDEST-GADT7-nim1-2 pDEST-GADT7-npr1-1 pDEST-GADT7-npr1-5 pDEST-GADT7-NPR1\(\Delta\)AKR pDEST-GADT7-NPR1\(\Delta\)AKR pDEST-GADT7-NPR1C521A pDEST-GADT7-NPR1C529A pGEX-2TK GST	This paper	N/A
pDEST-GADT7-AvrPtoB pDEST-GADT7-FQUS pDEST-GBKT7-AvrPtoB ₁₋₂₀₅ pDEST-GBKT7-AvrPtoB ₁₋₃₀₇ pDEST-GBKT7-AvrPtoB ₁₋₃₈₇ pDEST-GBKT7-AvrPtoB ₁₋₃₈₇ pDEST-GBKT7-AvrPtoB _{2-1.05} pDEST-GBKT7-AvrPtoB ₃₀₈₋₄₃₆ pDEST-GBKT7-AvrPtoB ₃₀₈₋₄₃₆ pDEST-GBKT7-AvrPtoB ₃₀₈₋₅₅₃ pDEST-GADT7-NPR1 ₁₋₂₈₀ pDEST-GADT7-NPR1 ₁₅₀₋₅₉₃ pDEST-GADT7-nim1-2 pDEST-GADT7-npr1-1 pDEST-GADT7-NPR1ΔAKR pDEST-GADT7-NPR1ΔAKR pDEST-GADT7-NPR1C521A pDEST-GADT7-NPR1C529A pGEX-2TK GST pDEST15 GST-AvrPtoB _{E3-LOF}	This paper	N/A
pDEST-GADT7-AvrPtoB pDEST-GADT7-NPR1 pDEST-GADT7-GUS pDEST-GBKT7-AvrPtoB ₁₋₂₀₅ pDEST-GBKT7-AvrPtoB ₁₋₃₀₇ pDEST-GBKT7-AvrPtoB ₁₋₃₈₇ pDEST-GBKT7-AvrPtoB ₁₋₃₈₇ pDEST-GBKT7-AvrPtoB _{23-LOF} pDEST-GBKT7-AvrPtoB ₃₀₈₋₄₃₆ pDEST-GBKT7-AvrPtoB ₃₀₈₋₅₅₃ pDEST-GBKT7-AvrPto pDEST-GADT7-NPR1 ₁₋₂₈₀ pDEST-GADT7-NPR1 ₁₅₀₋₅₉₃ pDEST-GADT7-nim1-2 pDEST-GADT7-npr1-1 pDEST-GADT7-NPR1ΔAKR pDEST-GADT7-NPR1C521A pDEST-GADT7-NPR1C529A pGEX-2TK GST	This paper	N/A

(Continued on next page)

Continued		
REAGENT or RESOURCE	SOURCE	IDENTIFIER
pCB302 35S:NPR1-GFP	Mou et al., 2003	N/A
pTA7002 Dex:Flag-AvrPtoB	This paper	N/A
pEG202 35S:Flag-AvrPtoB	This paper	N/A
pEG202 35S:Flag-AvrPtoB _{E3-LOF}	This paper	N/A
pEG202 35S:Flag-GUS	This paper	N/A
pLN615 Pfo-AvrPtoB	This paper	N/A
pLN615 Pfo-AvrPtoB _{E3-LOF}	This paper	N/A
Software and Algorithms		
Prism	GraphPad	ver 6; RRID: SCR_007370
ImageJ	NIH	ver 1.49a; RRID:SCR_003070

CONTACT FOR REAGENT AND RESOURCE SHARING

Further information and requests for resources and reagents should be directed to and will be fulfilled by the Lead Contact, Zheng Qing Fu (zfu@maibox.sc.edu).

EXPERIMENTAL MODEL AND SUBJECT DETAILS

Arabidopsis

All of the *Arabidopsis* [*Arabidopsis thaliana* (L.) Heynh.] transgenic lines and mutants were derived from Columbia (Col-0) ecotype unless otherwise noted. After stratification of seeds at 4°C for 3 days in the dark, *Arabidopsis* plants were grown in soil at 22°C with relative 70% humidity in a growth chamber (12 h light/12 h dark). For *in vitro* culture, surface sterilized seeds were sowed on plates containing 1/2 Murashige and Skoog (MS) basal salts and 1% sucrose, pH 5.7 solidified with 0.25% phytagel (Sigma-Aldrich) at 22°C under long-day conditions (16 h light/8 h Dark). Transgenic plants were generated by *Agrobacterium tumefaciens* (GV3101)-mediated transformation using the floral dipping method. The *Dex:Flag-AvrPtoB* and *Dex:Flag-AvrPtoB*_{E3-LOF} transformants were selected on 1/2 MS medium with 5 µM hygromycin B. The *NPR1-GFP/npr1-2* transgenic plants were reported previously (Mou et al., 2003). The *Dex:Flag-AvrPtoB* construct was also transformed into *NPR1-GFP/npr1-2* background in order to generate *Dex:Flag-AvrPtoB*; *NPR1-GFP/npr1-2* transgenic lines. All transgenic lines with a 3:1 segregation ratio of resistant:sensitive (in T₂) were examined in the T₃ generation to obtain homozygous transgene plants. Inducible expression of transgene was confirmed by immunoblot. The *Arabidopsis* mutants *npr1-2* (Cao et al., 1997), *npr1-3* (CS3802), *eds1-2* (Bartsch et al., 2006), *pad4* (Jirage et al., 1999), *ics1* (Wildermuth et al., 2001), *eds5* (Nawrath et al., 2002) and *fls2* (Salk_141277) were used in this study.

Nicotiana benthamiana

N. benthamiana was grown in greenhouses at 22°C with a long-day photoperiod (16 h light and 8 h dark).

Bacterial Strains

Pst DC3000, hrcC⁻ mutant, ΔavrPtoB mutant, ΔavrPtoBΔavrPto double mutant, P. fluorescens (Pfo), P. syringae pv maculicola (Psm) ES4326, DC3000 ΔavrPtoB mutant carrying AvrRpt2, and Psm ES4326 carrying AvrRpt2 strains were grown at 28°C on the King's B (KB) medium with appropriate antibiotics.

METHOD DETAILS

Plasmid Construction

Sequences of gene-specific primers used in this study are listed in Table S1. The amplified fragments by PCR in all constructs were analyzed by DNA sequencing to ensure that all sequences are validated.

The DNA sequences of the validated type III effector proteins from *Pseudomonas syringae* previously inserted into the entry vectors pDONR207 and/or pENTR/D-TOPO (Chang et al., 2005; Guo et al., 2009) were individually remobilized into the gateway destination vector pGBKT7 (Clontech) using Gateway (GW) LR Clonase II Enzyme Mix (Invitrogen) following manufacturer's instructions. The entire coding regions of NPR1 and GUS, which has similar molecular weight to NPR1, were cloned into the gateway destination vector pGADT7 (Clontech) by recombination, respectively. To make different truncations of AvrPtoB (AvrPtoB₁₋₂₀₅, AvrPtoB₁₋₃₀₇, AvrPtoB₁₋₃₈₇, AvrPtoB₃₀₈₋₄₃₆ and AvrPtoB₃₀₈₋₅₅₃) or NPR1 (NPR1₁₋₂₈₀ and NPR1₁₅₀₋₅₉₃), these truncated fragments were amplified by PCR using Phusion[®] DNA Polymerases (NEB) and introduced into the pDONR207 by BP clonase followed by recombination to enter the GW compatible destination vectors pGBKT7 or pGADT7. The NPR1ΔAKR fragment was generated using the overlap PCR method by two rounds of PCR amplifications. The N-terminal and C-terminal of NPR1 for making ΔAKR deletion constructs were

amplified using appropriate primers that add additional sequences homologous to the flanking regions, respectively. These two PCR products were purified and used as template in the second PCR using common primers. Full-length NPR1 Δ AKR products were cloned into aforementioned GW vectors. To generate various site mutations of AvrPtoB (AvrPtoB_{E3-LOF}) and NPR1 (*nim1-2*, *npr1-1*, *npr1-5*), amino acid substitutions within relative pDONR207 backbone were PCR amplified using PfuTurbo DNA Polymerase (Agilent) based on site-directed mutagenesis protocol (Stratagene). The desired nucleotide changes were designed in the middle region of the each complementary primer sequence. The PCR products were digested by DpnI (NEB) to remove template plasmid and the rest was transformed into Top10 *E. coli* by electroporation using Eppendorf Eporator[®]. Subsequently, these entry constructs were recombined with GW vectors as described above.

To make constructs for plant transformation or infection, the Flag-GW fragment was amplified from pEarlyGate202 and inserted into Xhol/Spel sites in pTA7002, yielding the homemade GW compatible vector designated as pTA7002_Flag-GW. The pDONR207-AvrPtoB and pDONR207-AvrPtoB_{E3-LOF} were then introduced into destination vector pTA7002_HA-GW to obtain the Dex:Flag-AvrPtoB and Dex:Flag-AvrPtoB_{E3-LOF} vector, respectively. For the cloning of 35S:HA-AvrPtoB (pEG201-AvrPtoB), pDONR207-AvrPtoB was transferred to the desired destination vector pEarlyGate201 overexpression vector by LR reaction. 35S:NPR1-GFP construct was designed using pCB302 binary vector as described previously (Mou et al., 2003). The pENTR/D-TOPO-GUS (Invitrogen) vector was linearized and subsequently cloned into pEG202 by recombination reaction to yield 35S:Flag-GUS (pEG202-GUS). To generate C-terminal HA fusion vector for *P. fluorescens* infection assays, the full-length AvrPtoB and AvrPtoB_{E3-LOF} ORF were amplified and sub-cloned into pENTR/D-TOPO vector. These entry vectors were then inserted into the GW vector pLN615 (Guo et al., 2009) by recombination to create Pfo-AvrPtoB and Pfo-AvrPtoB_{E3-LOF}, respectively.

For making constructs for recombinant protein expression, the coding sequence of NPR1 was amplified by PCR using gene-specific primers flanked by BamHl/Sall restriction enzyme sites and sub-cloned into pCRTM-Blunt II-TOPO vector (Invitrogen). After sequence confirmation, the NPR1 sequence flanked by BamHl/Sall restriction enzyme sites was ligated into pET-32a vector (Novagen) to yield the recombinant Trx-His₆-NPR1construct. To create GST-AvrPtoB and GST-AvrPtoB_{E3-LOF} vectors, the entry vectors mentioned above were cloned into pDEST15 by LR reaction.

Yeast Two-Hybrid Screens

The full length region of NPR1 was fused to N-terminal GAL4 DNA activation domain in the pGADT7 vector and was used to screen against homemade *Pseudomonas syringae* effector inventory containing type III effector proteins fused with N-terminal GAL4 DNA binding domain in pGBKT7. Then the *Saccharomyces cerevisiae* yeast strain Y187 transformed with pGBKT7-Effector plasmids was mated with the yeast strain AH109 transformed with pGADT7-NPR1 plasmids to suppress background activation. The pGADT7-GUS vector was used as negative controls. The healthy diploids on the double dropout (DDO) medium were subsequently selected and placed on quadruple dropout (QDO) medium at 30°C, according to the high-stringency selection protocol. The plasmids from positive clones were isolated and subsequently analyzed by DNA sequencing to ensure no mutations occurred. For spotting on the plates, $10 \, \mu l$ aliquots of yeast cell suspensions (OD₆₀₀=1.0, 0.1 and 0.01; from left to right) were applied. Yeast transformation, mating, interaction test and plasmid isolation were performed using the Yeast Protocols Handbook and Matchmaker GAL4TM Two-hybrid System 3 & Libraries User Manual (Clontech).

Yeast Protein Extraction

Yeast cells grown on selective media plates were suspended into liquid medium and incubated overnight at 30° C. 2 ml of cell culture was centrifuged and the pellet was re-suspended with $200 \,\mu$ l of 2 M LiAc on ice for 5 min. After centrifugation at $3000 \,\mathrm{rpm}$ for 5 min, the pellet was re-suspended with $200 \,\mu$ l $0.4 \,\mathrm{N}$ NaOH on ice for 5 min. The pellet was mixed thoroughly with $100 \,\mu$ l 2X Laemmli Sample Buffer (Bio-Rad) and boiled for 5 min. Then the supernatant containing yeast whole protein after removing debris by spin down was loaded onto a precast SDS-PAGE gel.

Recombinant Protein Purification

Recombinant GST-AvrPtoB, GST-AvrPtoB $_{E3-LOF}$ and Trx-His $_6$ -NPR1 proteins were heterologously expressed in *E. coli* OverExpressTM C41 (DE3) strain (Lucigen). Bacterial cells were grown in Luria Broth medium at 30°C until OD $_{600}$ reaches 0.4 \sim 0.6. The expression of the recombinant proteins was induced with 0.1 mM IPTG at 16°C overnight. The cell pellets were resuspended in BugBuster protein extraction reagent (Novagen) with 1 μ I/ml Benzonase Nuclease, 1 μ I/ml DNase, 1 mM PMSF, 1X cOmpleteTM EDTA-free protease inhibitor cocktail (Roche), 10 mM DTT and 10 μ M MG115 (Sigma-Aldrich). After two cycles of freezing and thawing followed by centrifugation, the supernatant was desalted with PBS buffer using PD-10 columns (GE Healthcare). The eluted protein mixture was incubated with glutathione resin (G-Biosciences) or MagneHisTM Ni-Particles (Promega) according to the technical manual. After repeated washes, the GST and His fusion proteins were eluted using 50 mM glutathione and 0.5 M imidazole, respectively. Purified proteins were alternatively dialyzed against 25 mM HEPES buffer pH 8.0 with 100 mM NaCl and 10 mM DTT using Slide-A-LyzerTM Dialysis Cassettes (ThermoFisher), and supplemented with 10% glycerol to store at -70°C until use.

GST Pull-Down Assay

The GST fusion protein isolation was carried out using the MagneGSTTM Protein Purification System (Promega). After cell lysis, 1 ml of GST and GST-AvrPtoB cell extracts were incubated with 10 µl MagneGSTTM particles (Promega) for 1 h at 4°C. After the immobilized beads were washed five times, equal amount of the Trx-His₆-NPR1-containing cell lysates were added to each sample followed by a

second incubation in the binding buffer (20 mM Tris-HCl, pH 7.5, 100 mM NaCl, 1 mM DTT, 1 mM PMSF, 1X cOmpleteTM protease inhibitor cocktail from Roche, 10 μ M MG115, 10% glycerol, 0.3% IGEPAL, 1% BSA) at 4°C for 4 h. The GST particles were recovered and washed five times with washing buffer (20 mM Tris-HCl, pH 7.5, 100 mM NaCl, 10% glycerol, 0.3% IGEPAL[®] CA-630). In the parallel pull-down assay by addition of SA, 200 μ M SA was applied in binding buffer and washing buffer. After washing, the subsequent elution was analyzed for the presence of Trx-His₆-NPR1. The bound proteins were eluted by addition of 2X Laemmli Sample Buffer (Bio-Rad) and 50 mM DTT followed by a heat treatment at 75°C for 10 min. Immunoblot was used for detection of Trx-His₆-NPR1 and GST fusion proteins with α -His (GenScript) and α -GST (GE Healthcare) antibodies.

Plant Protein Extraction and Immunoblotting

Plant tissues were sampled and ground in liquid nitrogen using 2010 Geno/Grinder® (SPEX). Total protein was homogenized in Protein Extraction Buffer [PEB; 50 mM Tris-HCl, pH 7.5, 1 mM EDTA, pH 8.0, 150 mM NaCl, 0.1% TritonTM X-100 (Sigma-Aldrich), 0.1% sodium deoxycholate (ThermoFisher), 0.5% IGEPAL® CA-630 (Sigma-Aldrich), 5% glycerol, 1 mM PMSF, 3 mM DTT, 1X protease inhibitor cocktail (Sigma-Aldrich), 1X PhosSTOP phosphatase inhibitor cocktail (Roche), 50 μM MG115 (Sigma-Aldrich)]. After centrifuged twice, the supernatants were collected, while protein concentration was determined using Bradford reagent (Bio-Rad). The sample was denatured with 5X sample buffer (250 mM Tris-HCl, pH 6.8, 6% SDS, 0.5 M DTT, 0.08% bromophenol blue, 30% glycerol) at 70°C for 10 min, run on a precast ExpressTM PAGE gel (GenScript) using NuPAGE® electrophoresis system, and subsequently transferred onto nitrocellulose membranes (GE Healthcare). For non-reduced conditions, protein was extracted in PEB without DTT and denatured with 5X sample buffer lacking DTT. Immunoblot assays were performed using primary antibodies [α-GFP (Clontech), α-HA-peroxidase (3F10, Roche), α-Flag® M2-peroxidase (Sigma-Aldrich), α-NPR1 (Agrisera), α-PR1 (Agrisera)] and secondary antibodies [a goat α-rabbit IgG-HRP (Agerisera), a goat α-mouse IgG-HRP (Santa Cruz Biotech) and a donkey α-goat IgG-HRP (Santa Cruz Biotech)] followed chemiluminescence detection using SuperSignal West Pico or Dura substrate (ThermoFisher). Immunoreactive proteins were visualized on a film by the SRX-101A Medical Film Processor (Konica). The membrane was stained with Ponceau S solution (0.1% Ponceau S and 5% acetic acid) to ensure equal protein loading.

Co-Immunoprecipitation (Co-IP) Assav

For Co-IP experiments using *N. benthamiana*, one gram of leaves was ground into fine powder in liquid nitrogen using a chilled mortar and pestle. Proteins were extracted with cold PEB in tubes and incubate on ice for 10 min with occasionally vortex. After centrifugation, the supernatants were filter through a 0.2 μ M filter and pre-cleared with blocked magnetic agarose beads for 5 min. The whole cell extracts were incubated with 25 μ I GFP-Trap®_MA beads (Chromotek) with gentle rocking for 4 h at 4°C. The conjugated beads were collected by a magnetic separation stand (Promega) and washed 3 times using 500 μ I PEB without MG115 and protease inhibitor cocktail. Precipitated samples were eluted with the addition of 2X Laemmli Sample Buffer (Bio-Rad) and 50 mM DTT by boiling for 5 mins. The bound HA-AvrPtoB protein was detected by α -HA immunoblots. 2% of the crude extracts were used as input control. For Co-IP assays in *Arabidopsis*, 2 g of leaves were sampled following the procedure described as above. The supernatants were pre-washed with protein A/G beads for 30 min. The protein samples were incubated with 25 μ I α -FLAG® M2 magnetic beads (Sigma-

pre-washed with protein A/G beads for 30 min. The protein samples were incubated with 25 μ l α -FLAG® M2 magnetic beads (Sigma-Aldrich) by gentle rotation for 4 h at 4°C. Then the beads were separated and washed 6 times extensively using washing buffer (50 mM Tris-HCl, pH 7.5, 1 mM EDTA, 150 mM NaCl, and 0.5% IGEPAL® CA-630). Samples were boiled with loading buffer for 5 mins before fractioned by SDS-PAGE.

Ubiquitination Assay

For the *in vivo* ubiquitination experiment, leaves of soil-grown plant were ground in reduced PEB containing 10 mM DTT, 10 mM iodoacetamide and 100 μ M MG115. The crude extracts were incubated and immuno-precipitated using GFP-Trap[®]_MA beads as described above. The bound proteins were eluted and analyzed using α -UBQ11 (Agrisera), α -GFP (Clontech) and α -Flag antibodies (Sigma-Aldrich).

Agrobacterium-Mediated Transient Assay

The $3\sim4$ -week-old *N. benthamiana* leaves were used in all experiments in this study. Different *Agrobacterium tumefaciens* GV3101 strains carrying indicated binary vectors were cultured in YEB medium with appropriate antibiotics. The *Agrobacterium* strains (a dilution of 1:100) were then added into new medium containing $100~\mu\text{M}$ acetosyringone and cultured at 30°C overnight. Bacteria were pelleted and resuspended in an induction buffer ($10~\text{mM}~\text{MgCl}_2$, 10~mM~MES, pH 5.7, and $100~\mu\text{M}$ acetosyringone). Cells were kept in induction buffer for 3 h and then infiltrated into the fully expanded leaves using a needleless syringe. The bacteria carrying expression vectors (HA-AvrPtoB, Flag-AvrPtoB, Flag-AvrPtoB_{E3-LOF}, Dex:Flag-AvrPtoB, NPR1-GFP, Flag-GUS, etc.) were infiltrated at an OD₆₀₀ of 0.3 and at OD₆₀₀ of 0.1 for the p19 construct. After co-infiltration, plants were immediately covered with a plastic dome for 24 h before the humidity dome was removed. The infiltrated leaves were harvested 2 days after infiltration and subjected to downstream experiments.

For inducible expression of *Dex:Flag-AvrPtoB*, plant leaves were spray with 10 μ M Dex (Sigma-Aldrich) in 0.01% Silwet L-77 2 days after agroinfiltration and sampled at indicated time points. For NPR1-GFP recovery assays, MG115 or Bafilomycin A1 (BioViotica) was co-infiltrated with the *Agrobacterium* strains.

Callose Staining and Quantification

Rosette leaves of 5-week-old plants were infiltrated with P. syringae pv tomato DC3000, Pst DC3000 $\Delta avrPtoB$ mutant, or Pst DC3000 $hrcC^-$ mutant at 10^8 cfu/ml (OD₆₀₀ = 0.2) and covered with humidity domes for 12 h. Leaves were detached and cleared in acetic acid/ethanol (1:3) for 6 h with several changes. Cleared leave were rinsed in 50% ethanol for 1 h, 30% ethanol for 1 h, water for 1 h, and finally with 150 mM K_2 HPO4 (pH 8.0) for 1 h. After destaining of chlorophyll and rehydration of leaves, the cleared samples were stained with 0.01% aniline blue in 150 mM K_2 HPO4 (pH 8.0) overnight in the dark. Leaves were rinsed in water and mounted in 50% glycerol, and examined under a fluorescence microscopy (Carl ZEISS Axiovert 200M) using a DAPI filter. The images were acquired using a constant setting with 1000 ms exposure time. The number of callose deposits was quantified using ImageJ software.

NPR1-GFP Distribution and Quantification

Rosette leaves of soil-grown 35S:NPR1-GFP/npr1-2 transgenic Arabidopsis plants were hand-infiltrated with buffer (10 mM MgCl₂), 0.2 mM SA, or bacterial at OD₆₀₀ = 0.2 for 12 h. GFP fluorescence in the abaxial surface of local leaves was detected by the aforementioned microscope with the FITC filter setup. GFP images were acquired by the AxioVision software using the same setting with 3000 ms exposure time. The number of nuclei with fluorescence in mesophyll and stomatal guard cells was quantified with ImageJ software.

Pathogenicity Tests

Bacteria were scraped from the plates, washed, serially diluted to the desired density with 10 mM MgCl $_2$. The $4\sim$ 6-week-old *Arabidopsis* grown in soil was used in this study as described above. A bacterial suspension was infiltrated into abaxial side of rosette leaves using a 1-ml syringe. After infiltration, the extra suspension on the leaf surface was removed. Plants were then placed in a growth chamber and covered by domes with high humidity until measuring bacterial growth. To determine bacterial multiplication, three leaf discs for each sample were pooled and at least six such samples were used for each data set (a total of 18 leaf discs at least). The samples were ground in 500 μ l of 10 mM MgCl $_2$ by Geno/Grinder, and serially diluted using 96-well plates. Several dilutions (20 μ l/each dilution) were plated on KB medium with the appropriate antibiotics. Bacterial colony forming units (cfu) were enumerated 2 \sim 3 days after incubation on plates at 28 $^{\circ}$ C.

For protein expression, cell wall callose deposition, GFP translocation, or RNA transcription experiments, bacterial (e.g., Pst DC3000, $hrcC^-$, $\Delta avrPtoB$, $\Delta avrPtoB\Delta AvrPto$, and $Pfo\ AvrPtoB$) cell density was typically adjusted to OD₆₀₀ = 0.2 (\sim 10⁸ cfu/ml). For protein expression in seedlings (Figure 3C), plants were submerged in bacterial (Pst DC3000, $hrcC^-$, $\Delta avrPtoB$) suspensions of OD₆₀₀ = 0.6. In bacterial virulence assays, the bacterium (OD₆₀₀ = 0.001) was infiltrated with or without 10 nM of DEX (Sigma-Aldrich) In the multiplication assays on the non-pathogenic Pst DC3000 $hrcC^-$ mutant, plants were sprayed with 3 μ M DEX in 0.01% Silwet L-77 6 h prior to syringe infiltration of $hrcC^-$ at OD₆₀₀ = 0.02. To assess the effect of AvrPtoB on flg22-trigged resistance, a combination of 10 nM DEX and 2 μ M flg22 peptides (GenScript) was infiltrated into leaves of the DEX inducible AvrPtoB transgenic plants for 2 days, and then plants were infiltrated with Pst DC3000 at OD₆₀₀ = 0.001. For SA treatments, plants were pretreated by spraying of the plant leaves with a combination of 0.3 M of sodium salicylate solution (Sigma-Aldrich) and 3 μ M DEX in 0.01% Silwet L-77 for 2 days before infiltration of Psm ES4326 at OD₆₀₀ = 0.001. In SAR test, plants were sprayed by 3 μ M DEX 6 h prior to infiltration of Psm ES4326 carrying AvrRpt2 (OD₆₀₀ = 0.002) in two lower leaves. After 2 days, three upper leaves were challenged with virulence Psm ES4326 at OD₆₀₀ = 0.001.

Induction of AvrPtoB in Minimal Medium

The AvrPtoB and AvrPtoB $_{E3-LOF}$ were cloned into aforementioned pLN615, carrying a C-terminal HA-tag. The clones were transformed into *P. fluorescens*. Bacteria were grown onto KB agar media plates overnight and resuspended in minimal medium (7.8 mM ammonium sulfate, 50 mM potassium phosphate, 1.7 mM sodium chloride, 1.7 mM magnesium chloride, 10 mM mannitol and 10 mM fructose, pH 5.7) at an OD $_{600}$ of 0.02 . After incubation with shaking in 28°C overnight, 3 mL of each cell culture was centrifuged at room temperature for 3 min at a speed of 10,000 rpm. The pellet was resuspended thoroughly in 100 μ l 2X Laemmli Sample Buffer (Bio-Rad) and boiled for 5 min. Then 20 μ l of supernatant after spin down was loaded onto a precast SDS-PAGE gel.

Gene Expression Analysis

Arabidopsis leaves of CoI-0 wild type and npr1-2 mutant plants were hand-infiltrated with Pst DC3000, $\Delta avrPtoB$ mutant or $hrcC^-$ mutant at OD₆₀₀ = 0.2 in 10 mM MgCl₂. Total RNA was isolated using RNeasy Plant Mini Kit (Qiagen) according to the manufacture's manual. Before RNA elution, RNase-free DNase was added to remove contaminated genomic DNA at room temperature. RNA was quantified by BioPhotometer® D30 (Eppendorf), separated in agarose gel by electrophoresis and visualized using Gel DocTM XR+ Gel System (Bio-Rad). $2\sim5$ μg of total RNA was subjected to synthesize the first-strand cDNA using SuperscriptTM III First-Strand Synthesis System (Invitrogen). Each cDNA sample was diluted 1:10 and then used as template. For semi-quantitative reverse transcription (RT)-PCR analysis, 2 μl of diluted sample was applied to PCR amplification using GoTag® Green Master Mix (Promega).

In quantitative real-time (qRT)-PCR assay, PCR was set up using 96-well microplates (Axygen) with SYBR Green PCR Master Mix (Applied Biosystems) in a volume of 20 μ l. The qRT-PCR assays were conducted using with a 7300 real-time PCR system and 7300 system SDS software (Applied Biosystems). Each sample was performed in triplicate. The reference gene $eEF-1\alpha$ was used as an internal control to normalize the experimental data. The threshold cycle (Ct) was automatically determined for each reaction in the system. The comparative Ct method with Δ Ct = Ct (Reference) – Ct (Sample) was normalized to internal control. The value for



each data point was calculated by $2^{\Delta Ct}$. All PCR experiments were repeated at least twice, and representative results are shown. The gene-specific primer sets are provided in Table S1.

QUANTIFICATION AND STATISTICAL ANALYSIS

In all quantification experiments, the relative intensities of immunoblotting band, numbers of callose deposits and nuclear GFP signal were processed and quantified with Image J software (National Institutes of Health). For statistical analysis, the GraphPad Prism 6.0 software (GraphPad Software, Inc.) and Microsoft Office Excel 2010 were used in this work. Data are shown as mean \pm SD (or \pm SD) indicated in all figure legends. Numbers of sample and experimental repeats are indicated in figure legends. In Figures 4A and 6B, sample number (n) means the number of individual leaves. Otherwise, n indicates the number of biological replicates for each data point. Statistics were performed using analysis of variance (ANOVA) tests with Tukey's or Sidak's comparisons with 95% confidence (p < 0.05) or multiple t tests with different significance levels (** p < 0.01; *** p < 0.001). Details are shown in figure legends.